

HYDROGEOCHEMICAL CHARACTERIZATION OF GLACIAL-FED SURFACE WATER RESOURCES IN THE CATCHMENT AREAS OF UPPER INDUS BASIN



by

AMMAR YASIR

M.Phil. Hydrogeology

Department of Earth Sciences
Quaid-I-Azam University, Islamabad



2023

CERTIFICATE


It is certified that **Mr. Ammar Yasir S/o Haji Ali Madad (Registration No. 02112013006)** carried out the work contained in this dissertation under my supervision and accepted in its present form by Department of Earth Sciences as satisfying the requirements for the award of **M.Phil Degree in Hydrogeology**.

RECOMMENDED BY

Dr. Faisal Rehman
Assistant Professor/Supervisor



Dr. Aftab Alam
External Examiner



Dr. Aamir Ali
Chairperson



DEPARTMENT OF EARTH SCIENCES
QUAID-I-AZAM UNIVERSITY
ISLAMABAD

ACKNOWLEDGMENTS

All praise and gratitude are due to the omnipotent **Allah**, who bestowed upon me the enlightenment and fortitude to complete my research obligations. All respect to holly prophet **Hazrat Muhammad (P.B.U.H.)**, the last prophet and ideal role model for mankind.

My research adviser and mentor, **Dr Faisal Rehman** has my utmost respect and appreciation for his extensive mentoring and oversight of my M.Phil. dissertation. He has been a consistent source of inspiration and enthusiastic support. I am privileged to thank his supervision since I was able to complete my thesis because of his kind benevolence and expert guidance.

I am unable to adequately communicate my appreciation to my family members. I want to convey my appreciation to my parents., whose love and advice have accompanied me in all my endeavors and wherever I am in the globe. They are the most exemplary role models and my most devoted mentors.

I am grateful to the department of earth sciences, QAU for enabling me to pursue my Master's degree. Special thanks to **Dr Abbas Naseem** department of Earth Sciences QAU for support and help throughout.

AMMAR YASIR

ABSTRACT

The current study focuses to examine the Physio-chemical parameters of the glacially-fed water resources in the elevated areas of Gilgit-Baltistan, Pakistan. The glacially fed streams are the primary source for drinking and irrigation in the entire region. The evaluation of quality of such streams is particularly important because it helps to understand the geochemical processes that take part in changing the geochemistry of water on a regional basis. In this research work, total 40 water samples from different glacier-fed streams were obtained following the standard practices. The in-situ testing of all the field samples were carried for temperature, pH, TDS, and Conductivity by using different apparatuses. Later, the water samples were brought to the laboratory to perform the other major geochemical tests for characterization following standard procedures. The tests data of the geochemical parameters for all the water samples collected from the study region was tabulated and the variation in the physio-chemical parameters including Conductivity, Turbidity, pH, TDS, Hardness, Ca^{2+} , K^+ , Mg^{2+} , Na^+ , Cl^- , SO_4^{2-} , NO_3^- , Pb, Cd, Cu, Zn, Fe, Mn, As, Cr and Hg was measured and analyzed their fitness for drinking and irrigation. To meet the study objectives different hydro-chemical and hydro-geostatistical analyses including WQI, HPI, Gibbs Plot, Piper Plot, Ionic ratios and irrigation suitability water quality data were compared to WHO's worldwide water quality standards. The water quality of the study area is classified as excellent (50%), good (32.5%), and medium (17.5%) based on WQI values. Heavy metal pollution index (HPI) values are found far below the critical values, indicating safe for human consumption in terms of heavy metal pollution. Furthermore, the study found water quality was found suitable for irrigation purposes in terms of all irrigation quality parameters. According to Gibbs plot and ionic ratios, rock weathering is dominant especially carbonate weathering with little contribution of

silicate rocks in controlling the water chemistry. Piper plot for study area also revealed carbonate rocks as dominant geochemical facies and classified the water types as Ca-HCO₃, Mixed Ca-Mg-Cl, Ca-Cl, and Ca-Na-HCO₃ type.

Table of Contents

ACKNOWLEDGMENTS	III
ABSTRACT.....	IV
LIST OF FIGURES	X
LIST OF TABLES.....	XII
NOMENCLATURE	XIII
1 INTRODUCTION	14
1.1 BACKGROUND.....	14
1.2 PROBLEM STATEMENT	18
1.3 RESEARCH OBJECTIVES	18
1.4 THESIS STRUCTURE	19
2 LITERATURE REVIEW	21
3 STUDY AREA.....	28
3.1 GILGIT RIVER BASIN.....	29
3.2 CLIMATE OF THE AREA	30
4 RESEARCH METHODOLOGY	32
4.1 FIELD WORK	32
4.1.1 Water Sampling	32
4.2 DETERMINATION OF PHYSICAL PARAMETERS.....	32
4.2.1 Determination of Temperature.....	32
4.2.2 Determination of pH	33
4.2.3 Determination of Electric conductivity.....	33
4.2.4 Determination of turbidity	33
4.2.5 Determination of Total Dissolved Solids (TDS)	33
4.3 DETERMINATION OF CHEMICAL PARAMETERS	34

4.4	DETERMINATION OF ANIONS	34
4.4.1	Chloride (Cl^-)	34
4.4.2	Sulfate (SO_4^{2-}).....	35
4.4.3	Phosphate (PO_4^-)	35
4.4.4	Nitrate (NO_3^-).....	36
4.4.5	Carbonate (CO_3^-) and Bicarbonate (HCO_3^-)	36
4.5	DETERMINATION OF CATIONS	37
4.5.1	Sodium and Potassium.....	37
4.5.2	Calcium and Magnesium	37
4.5.3	Hardness.....	38
4.6	DETERMINATION OF HEAVY METALS.....	39
4.7	ANALYSIS AND EVALUATION	40
4.7.1	Hydro-Geochemical Analysis.....	41
5	RESULTS AND DISCUSSIONS	42
5.1	WATER CHEMISTRY	42
5.2	WATER CHEMISTRY OF THE UNDER-STUDY REGION	43
5.3	ION CHARGE BALANCE ERROR	43
5.4	CHARACTERIZATION OF INDIVIDUAL HYDRO-GEOCHEMICAL PARAMETERS	44
5.4.1	pH.....	45
5.4.2	Turbidity	46
5.4.3	Total Dissolved Solid (TDS)	47
5.4.4	Electric Conductivity	48
5.4.5	Total Hardness	49
5.5	CATIONS.....	50

5.5.1	Sodium (Na^{2+}).....	50
5.5.2	Potassium (K^{+}).....	51
5.5.3	Calcium (Ca^{2+}).....	52
5.5.4	Magnesium (Mg^{2+}).....	52
5.6	ANIONS.....	53
5.6.1	Chloride (Cl^{-}).....	53
5.6.2	Bicarbonate (HCO_3^{-}).....	56
5.6.3	Nitrate (NO_3^{-}).....	57
5.6.4	Sulfate (SO_4^{2-}).....	58
5.6.5	Phosphate (PO_4^{2-}).....	59
5.7	EVALUATION OF WATER QUALITY	64
5.7.1	Water Quality Index (WQI).....	64
5.7.2	Heavy Metal Pollution Index (HPI)	69
5.8	WATER QUALITY ASSESSMENT FOR IRRIGATION PURPOSES	72
5.8.1	Sodium Absorption Ratio (SAR).....	72
5.8.2	Residual Sodium Carbonate.....	73
5.8.3	Magnesium Hazard (MH)	74
5.8.4	Sodium Percentage ($\text{Na}^{\circ}\%$).....	75
5.8.5	Permeability Index (PI).....	75
5.9	THOSE REPORTED IN LITERATURE	77
5.10	HYDRO-GEOCHEMICAL PROCESSES.....	81
5.10.1	Gibs Plot.....	81
5.11	CHARACTERIZATION OF GEOCHEMICAL FACIES AND HYDRO CHEMICAL WATER TYPES	83
5.11.1	Piper Graphical Plot.....	83

5.12	IONIC RATIOS.....	86
6	CONCLUSION	90
7	RECOMMENDATIONS	92
	BIBLIOGRAPHY	93
	APPENDIX.....	104
	VITA.....	105

LIST OF FIGURES

Fig 3. 1 Sampling Locations of the Study Area.....	29
Fig 5. 1 Graph of pH for the Monitored Values of Physiochemical Parameters and Their Comparison with WHO limits.....	46
Fig 5. 2 Graph of Turbidity for the Monitored Values of Physiochemical Parameters and Their Comparison with WHO limits.....	47
Fig 5. 3 Graph of TDS for the Monitored Values of Physiochemical Parameters and Their Comparison with WHO limits.....	48
Fig 5. 4 Graph of Conductivity for the Monitored Values of Physiochemical Parameters and Their Comparison with WHO limits.....	49
Fig 5. 5 Graphs of Hardness for the Monitored Values of Physiochemical Parameters in Contrast to the WHO's recommended levels	50
Fig 5. 6 Graph of Sodium (Na^{2+}) for the Monitored Values of Physiochemical Parameters in Contrast to the WHO's recommended levels	51
Fig 5. 7 Graph of Potassium (K^{+}) for the Monitored Values of Physiochemical Parameters in Contrast to the WHO's recommended levels	51
Fig 5. 8 Graph of Calcium (Ca^{2+}) for the Monitored Values of Physiochemical Parameters in Contrast to the WHO's recommended levels	52
Fig 5. 9 Graph of Magnesium (Mg^{2+}) for the Monitored Values of Physiochemical Parameters in Contrast to the WHO's recommended levels	53
Fig 5. 10 Graph of Chloride (Cl^{-}) for the Monitored Values of Physiochemical Parameters in Contrast to the WHO's recommended levels	54
Fig 5. 11 Graph of Bicarbonate (HCO_3^{-}) for the Monitored Values of Physiochemical Parameters in Contrast to the WHO's recommended levels	56

Fig 5. 12 Graph of Nitrate (NO_3^-) for the Monitored Values of Physiochemical Parameters in Contrast to the WHO's recommended levels	57
Fig 5. 13 Graph of Sulfate (SO_4^{2-}) for the Monitored Values of Physiochemical Parameters in Contrast to the WHO's recommended levels	58
Fig 5. 14 Graph of Phosphate (PO_4^{2-}) for the Monitored Values of Physiochemical Parameters in Contrast to the WHO's recommended levels	59
Fig 5. 15 Graphs for the Monitored Values of Physiochemical Parameters in Contrast to the WHO's recommended levels, (A) Cd, (B) Pb, (C) Zn, (D) Fe, (E) Mn, (F) As, (G) Cr and (H) Hg.	61
Fig 5. 16 The Water Quality Index Value of the Water Samples using GIS Map.....	68
Fig 5. 17 Graph of The Water Quality Index Value of the Water Samples.....	68
Fig 5. 18 Heavy Metal Pollution (HPI) Values for the Collected Water Samples	71
Fig 5. 19 Physical Properties of the Water Samples Compared to those in Published Research.....	78
Fig 5. 20 Chemical Characteristics of the Water Samples Compared to Those in Published Research	79
Fig 5. 21 Heavy metals of the water samples compared to those in published research.	80
Fig 5. 22 Gibbs Plot Showing (a) TDS vs $\text{Na}^+/\text{Na}^+ + \text{Ca}^{2+}$, (b) TDS vs $\text{Cl}^-/\text{Cl}^- + \text{HCO}_3^-$ Showing Dominance of Rock Weathering	83
Fig 5. 23 Piper Diagram for Surface Water of the Study Region.....	85
Fig 5. 24 Scatter Plots Showing the Variability in Ionic Concentrations of Water Samples	88

LIST OF TABLES

Table 4.1 List of Equipment Used in Field for the Measurement of Physio-Chemical Parameters.....	34
Table 4.2 List of Laboratory Methods Used in Measurement of Anions and Cations	39
Table 4.3 List of Laboratory Methods Utilize for the Measurement of Concentration of Heavy Metals for Collected Water Samples.....	40
Table 5.1 Values of Physiochemical Parameters in Water Samples, Compared to Standard Acceptable Ranges.....	55
Table 5.2 Hydrogeochemical parameters of individual water sample and their concentration in the study area	62
Table 5.3 Heavy metal concentration in ($\mu\text{g/L}$) for individual water sample of the study area.....	63
Table 5.4 Relative Weight of Physic-Chemical Parameters.....	66
Table 5.5 Categorization of water quality status based on WQI value (after Adimalla et al., 2019)	67
Table 5.6 Parameters for HMs in surface waters based on (WHO, 2017) recommendations for potable water.....	71
Table 5.7 Calculated Irrigation Water Quality Indices for the Region.....	76
Table 5.8 Suitability of Surface Water for Irrigation Based on Various Classifications	77

NOMENCLATURE

Symbol	Description
EC	Electric Conductivity
GIS	Geographic Information System
HMs	Heavy Metals
HPI	Heavy Metal Pollution Index
ICBE	Ion Charge Balance Error
LIB	Lower Indus Basin
MH	Magnesium Hazard
PI	Permeability Index
RSC	Residual Sodium Carbonate
SAR	Sodium Absorption Ratio
TDS	Total Dissolved Salts
TH	Total Hardness
UIB	Upper Indus Basin
WHO	World Health Organization
WQC	Water Quality Class
WQI	Water Quality Index

1 INTRODUCTION

1.1 BACKGROUND

Water is the most common and abundant substance on the planet earth. Fresh water makes up only 2.53% of the total, with the rest being salt water. Glaciers with permanent snow cover store around a third of the world's water. The remaining freshwater is spread regionally. The Earth, with its numerous and abundant living forms, including nearly six billion humans, is facing many social, economic and natural resource crises. The water crisis (quantity and quality) is at the heart of human survival, as well as the survival of our planet (UN WWAP, 2003). This issue will get more complicated in the future as a result of climate change, which promotes glacier melting, and an intensification of the water cycle, which may result in more floods and droughts. (Huntington, 2006). All indicators indicate that it is worsening and will continue to worsen unless immediate action is taken. When we talk about water quality, we're talking about its physical, chemical, and biological parameters based on the standards of its usage. Degradation of water occurs primarily as a result of changes in its quality parameters beyond natural variability caused by the addition or removal of various substances. The two most influential processes which affect water quality are human activities (or "anthropogenic" effect) and geogenic processes (natural processes). This includes the water's origin, the amount of evaporation that took place, the rocks and minerals that it came into contact with (i.e., the geological and mineralogical properties of the watershed), the occurrence of geological events, the water's velocity and the direction in which it was exposed to reactive elements, and the amount of time that it spent in contact with those elements. Water quality is affected by a variety of external pollution sources, including those used in agriculture, industry, and the household (Dinka et al., 2015).

The most significant factors leading to unanticipated, terrible, and dangerous outcomes are those with an anthropogenic distribution. These include the release of sewage into rivers, the use of unsuitable landfills, the transformation of land, and the impact of air deposition on global warming (Shabbir & Ahmad, 2015). Since water quality has a direct impact on all forms of life, scientists have been paying more attention to it in recent years (Kavurmaci & Üstün, 2016). Water contaminated by sewage pipes is not fit for human consumption and can't be used in food production, manufacturing, or any number of other applications. It is critical for human societies to have access to clean and fresh water, but environmental degradation is threatening the quality of land's water supplies (Terrado et al., 2010). Industrial and urban wastewaters, together with agricultural runoff, are major contributors to the pollution of surface water bodies. Because of the importance of understanding the hydro-morphological, hydro-chemical, and hydrobiological features of these water sources, an effective, long-lasting system is required. Surface water quality estimate assessment, based on the use of standardized rules and recommendations provided by the appropriate authorities, may help keep tabs on other significant shifts, such as regional and temporal variations.

As much as human activity affects water quality, geogenic elements (such as water-rock interaction) are just as important. Most people think of sewage or industrial waste matter running out of a discharge pipe when they hear the term "water pollution," and it's true that many toxic compounds are introduced into water systems as a result of human activity. The contact between rocks and water may also liberate minerals and metals, which can then be carried by runoff into lakes, rivers, or leach into ground aquifers, contaminating those bodies of water (William et al., 2005). Overall water quality is significantly impacted by the region's geological setting. The dominating rock formations in a region often dictate the physiochemical conditions of surface and underground waters. Water quality varies greatly across time and space as a result of

the dissolving of different minerals from diverse rock formations, which has serious consequences for human health and the environment. Additionally, it is now well accepted that weathering of altered zones in various geological units is a crucial process influencing the properties of water supplies. This process is also to blame for the many health problems experienced by local communities that rely on these water sources for drinking, household, and agricultural use.

In earth's crust many naturally occurring metals are found, and their composition varies by location, resulting in spatial differences in concentrations (Khan, et al., 2019; Khlifi & Hamza-Chaffai, 2010). On the basis of researched related activities and technology, heavy metals caused a serious change in geochemical processes. A number of harmful effects on human health may result from the slow but steady accumulation of these heavy metals in plant tissue. Heavy metal concentrations in drinking water still regularly exceed guidelines established by regulatory agencies in many countries, despite the rapid development of new technologies. The public and medical community are increasingly worried about the presence of heavy metals including chromium, cadmium, nickel, lead, arsenic, zinc, and mercury in their drinking water (Rehman et al., 2018). The accumulation of heavy metals like lead, mercury, and arsenic in the body over time is known to have negative health effects. There are several ways in which heavy metals may enter the body, including via ingestion (eating contaminated food), inhalation (breathing polluted water or air), and skin contact. Ground and surface water in Pakistan have been found to contain heavy metals like cadmium, arsenic, lead, and mercury (Rehman Qaisar et al., 2018). This necessitates a study of the threats posed by heavy metals to potable water supplies. Accurate predictions of exposure concentrations and chemical intakes are an important element of this process, as are the characterization of physical settings, the identification of possible exposure populations and routes, and the prediction of exposure

concentrations. There are serious health risks associated with exposure to heavy metals, and the symptoms experienced are quite variable.

Assessing water quality is a standard practice in the study, planning, and administration of water supplies. Rapid urbanization, industrialization, and agricultural activities all contribute to a rise in the risk of soil and water contamination, making this an increasingly pressing issue. For reasons including but not limited to public health (drinking or domestic use), agriculture, industry, fishing, recreation, tourism, and the protection of aquatic ecosystems, water quality monitoring is essential. Understanding the water quality condition and the processes influencing water quality is crucial for Integrated Water Resource Management (IWRM) activities within the watershed (Dinka et al., 2015; R. N. Tiwari, 2011).

The northern parts of Pakistan rely on water from glaciers, springs, lakes, and ponds to provide their most basic requirements. Most of the lakes are at an elevation of 2133.59 m above sea level, making them what are known as high-altitude glacier lakes (H. Khan & Baig, 2017). Sea levels fluctuate throughout time and space owing to factors like soil erosion, wind tide, glacial impact, and other natural catastrophes, thus we assumed height in respect to the surrounding lowland, which is of course changeable, or elevation in reference to the land, which is potentially deceptive. The primary environmental difference between high altitude and lowland ecosystems is height, which is characterized by cold temperatures, snow peaks, glacial lakes, alpine vegetation, and unique high-altitude biodiversity (Mani, 1986). It's safe to assume that the glaciers that flood the alpine lakes in Gilgit and its five adjacent regions are located at rather high elevations (Iturrizaga, 2005). The downstream running water from these lakes is used as drinking water as well as for irrigation purpose by the people. Without any appropriate mechanism, people exploit these lakes for their socioeconomic

benefits. Consequently, the water in these natural waterways is polluted by a variety of naturally occurring and man-made pollutants.

1.2 PROBLEM STATEMENT

In the northern regions of Pakistan, glaciers, lakes, springs, and ponds are the primary and most reliable sources of water. The people of Gilgit Baltistan rely on these high-altitude glaciers and lakes for their socio-economic requirements. Water for drinking and agricultural is provided by these sources. It is reported that, the water of the glacial streams and rivers in the region is contaminated as a result of faulty landfill systems and management, as well as a lack of environmental awareness among the local residents and visitors. Because of this, most of the water sources in these areas have seen a decline in quality and are now a potential source of water-borne diseases. No detailed studies on the water of glacial fed streams of Gilgit Baltistan have ever been conducted regarding characterization of physio-chemical and heavy metals contamination. Therefore, present study is supposed to investigate the suitability of these glacially fed stream waters for both drinking and agricultural purposes. In this regard different hydro-chemical and hydro-geostatistical analysis can be done by using various statistical approaches.

1.3 RESEARCH OBJECTIVES

- i. To analyze water samples from several Nullahs, rivers, and springs in Gilgit Baltistan to calculate the levels of various physiochemical parameters and to compare these results to World Health Organization (WHO) guidelines.
- ii. Determine the quality status of the water samples that have been analyzed and assign them a score using the water quality Index (WQI) method.

- iii. Determine the concentration of heavy metal ions in contemplated water resource, estimate their spatial distribution and assess their adverse effects on human health.

1.4 THESIS STRUCTURE

The thesis consists of seven chapters. A brief detail of each chapter is given below;

- **Chapter 1** depicts an overview of water resources and their degradation in terms of geogenic and anthropogenic impacts. It also enlightens the evaluation of water quality for human consumption in terms of its physio-chemical parameters.
- **Chapter 2** gives a detailed literature and methodologies adopted for water quality evaluation studies and geochemical characterization of surface and underground water resources around the globe.
- **Chapter 3** provides details about the geographic location, climate, water resources and sampling locations of the study area.
- **Chapter 4** includes detailed discussion of methodology adopted for the study. It includes the field and laboratory testing of physio-chemical parameters of the collected water samples. This chapter represents information about the equipment used and laboratory testing methods to determine the concentration of physio-chemical parameters of the samples.
- **Chapter 5** discusses in depth the geo-chemical and geo-statistical analysis that was used to the water quality index (WQI) in order to determine its suitability for human consumption and water quality parameters for irrigation in the research area. Geochemical mechanisms that regulate the water chemistry of a whole area are also identified. The Gibbs plot, Piper plot, and ionic ratios were used for this purpose.
- **Chapter 6** presents a brief conclusion of the research work.

- **Chapter 7** presents and proposes suggestions and recommendations for the future work.

2 LITERATURE REVIEW

In order to evaluate the quality of potable water and detect possible pollutants in a wide range of surface and subsurface water resources, researchers have used a wide array of methods and approaches. To have a comprehensive knowledge of the elements that contribute to surface water and groundwater pollution, it is of the highest importance to characterize the source of the contamination. Anthropogenic and natural processes may be the most significant contributors to contamination of water bodies. To explain the necessity of undertaking the current research, a brief literature analysis of analogous hydro-geochemical investigations done on similar types of surface and subsurface waters in Pakistan and other areas of the world has been reviewed.

Rehman Qaisar et al., 2018 conducted an in-depth study of the geochemical composition of water in the sub-catchment regions of Pakistan's Lower Indus Basin (LIB) and Upper Indus Basin (UIB), including its geographical variance, source identification, and quality evaluation. They found that IRB has a pH that is much higher than the global average, making it an alkaline substance. Wider TDS values were also detected in LIB, which had a higher standard deviation than global mean values, pointing to semiarid climates and increased human interference. The primary cation and anion concentrations are as follows: $\text{Ca}^{2+} > \text{Na}^{2+} > \text{Mg}^{2+} > \text{K}^+ > \text{Na}^+$ and $\text{HCO}_3^- > \text{SO}_4^{2-} > \text{Cl}^- > \text{NO}_3^-$. In the sub-catchments, statistical analysis of ionic concentrations reveals a substantial positive co-relation between Ca^{2+} and SO_4^- , Mg^{2+} and SO_4^- pairings, proving that sulphate mineral dissolution and pyrite oxidation are the most typical sources of SO_4^- . The NO_3^- and Ca^{2+} , NO_3^- and Mg^{2+} , and NO_3^- and Na^+ couples all have high positive correlations, according to statistics. They used the Gibbs plot to examine the water chemistry and control mechanism in their investigation. Weathering of rocks has a significant impact on the IRB's water's geochemistry, with evaporites dissolving making a modest contribution. To determine the current geo-chemical facies, the Piper

trilinear diagram, mixing diagrams, and ionic ratios are also displayed. All of these figures illustrate that carbonate weathering is dominant in influencing the geochemistry of water in the IRB catchment regions, with varying degrees of silicate weathering. From the standpoint of main ions, the water in the region meets the WHO permitted criteria for drinking, however for irrigation, the majority of the collected water samples indicated excellent and good levels, with only a few samples falling below permissible and dubious limits.

S. Li & Zhang, 2008 investigated the geographical distribution of key ion composition and their governing variables in the upper Han River basin of China's water geochemistry. The water in the basin is mildly alkaline, with low TDS and minimal mineralization, according to the researchers. The geochemical and anthropogenic processes were quantified using statistical analysis of co-relation matrices and Principal Component Analysis (PCA). This study found Ca^{2+} and Mg^{2+} as the most common cations, whereas HCO_3^- and SO_4^- are the most common anions. There is a substantial correlation between EC and TDS. The co-relation between HCO_3^- , Ca^{2+} , and Mg^{2+} was likewise positive. Only Na^+ and K^+ have a considerable co-relation. The substantial link between EC, TDS, Ca^{2+} , Mg^{2+} , and HCO_3^{2-} , which indicates carbonate weathering, is demonstrated using PCA analysis. The nature of NO_3^{2-} in the third component suggests human inputs, mineralization, and atmospheric deposition, whereas the connection between Na^{2+} , K^+ , Cl^- , and SO_4^{2-} in the second component indicates weathering of silicate and evaporites minerals. The basin has good water quality, based on spatial variance in total water quality and comparisons to WHO and Chinese drinking water criteria. Overall, they determined that weathering of carbonate and silicate rocks, as well as anthropogenic activities, influence the principal ion chemistry of the upper Han River basin, with evaporites providing a modest contribution.

Heba Abd El-Aziz Abu-bakr, 2021 performed study in Qena, Egypt, in order to assess the suitability of Nile Valley groundwater for human consumption and agricultural use, Egypt and its borders. The area's hydro-chemical condition was assessed using the Piper diagram, Gibbs plot, and Wilcox irrigation water quality indicators. The researcher employed basic descriptive and multivariate statistical analysis to determine the co-relation coefficients among the nine estimated water parameters for the statistical study. To forecast groundwater salinity in terms of electric conductivity, a regression analysis is used. The Kriging approach, which is based on a variogram model and was utilized by the researcher to improve the groundwater monitoring network in the study region, which determines the spatial distribution of groundwater quality. According to the Piper diagram, 74 percent of hydro-chemical faces represent NaCl water type, whereas 16.5 percent, 9.35 percent, and 4.32 percent of hydro-chemical faces reflect CaNaHCO_3 , Ca-Mg-Cl, and Ca-Cl water type, respectively. The Gibbs plot revealed that the majority of the samples fell within the rock and evaporation dominance zones. The water samples range from excellent to mediocre quality when viewed through the lens of several irrigation indices and the Wilcox diagram. Basic descriptive statistics, such as graphical displays, histograms, and probability plots, are generated hydro-geo-statistically to describe the data distribution, spreading of data, frequency of values, normalcy, and homogeneity of the samples. Electric Conductivity (EC) was shown to have a direct relationship with quantities of (pH, Ca^{2+} , Mg^{2+} , K^+ , Cl^- , SO_4^- , and HCO_3^-) in the regression analysis.

Fatima et al., 2022 investigated the impact of pollution on glacier streams and surface water supplies in Gilgit Baltistan's Basho Valley Skardu area. His research was based on laboratory examination, statistical methodologies, and the geographical distribution of main pollution indicators such as physic-chemical, metals, and microbiological factors. Physic-chemical, metals, and microbiological factors all have

their own WQI. Principal Component Analysis and correlation matrix are used for statistical analysis on normalized data. The spatial distribution of physic-chemical elements, metal, and microbiological factors is interpolated using inverse distance weighting, and the WQI values are interpolated using the inverse weight method (IDW). It was found that the spatial distribution of physicochemical characteristics and heavy metals was different at the eastern and southern ends of the study area, suggesting that there was more than one source of pollution in those areas. Using principal component analysis, the water quality index (WQI), and spatial distribution by means of the inverse distance weighting (IDW), it is determined that the water quality is exceptional with respect to its physicochemical features. In terms of heavy metals, alarmingly, 91 percent of the samples are deemed unsafe for consumption. Based on microbiological characteristics, 52 percent of the total samples are unsafe for drinking, surpassing WHO recommendations.

Zanotti et al., 2019 carried out research into the quality of surface and subsurface water in the Oglio river basin in Italy. 270 water samples were collected from 68 monitoring points. Water quality data is gathered by laboratory examination, and a multivariate method of factor analysis called positive matrix factorization (PMF) is used to determine the primary hydro-chemical properties and processes that influence them. Positive Matrix Factorization is a multivariate statistical methodology targeted at source identification that was developed expressly to deal with environmental data and manage its uncertainty and dispersion. The results of PMF are compared to those of a typical multivariate statistical analysis of factor analysis in terms of both factor profiles and their geographical distribution using a GIS technique in this study's analysis. Isotope analysis results are often utilized to validate PMF data and provide support for interpretation. Positive Matrix Factorization finds five separate components that indicate major aspects and natural and anthropogenic processes that impact the research

region, according to the findings: 1) irrigation surface water, 2) groundwater subjected to advanced reducing processes, 3) groundwater subjected to early reducing processes, 4) groundwater residence duration, and 5) the impacts of agricultural land use on both groundwater and surface water.

Jeelani et al., 2011 conducted time series research in Kashmir, Western Himalaya, to better understand the hydrogeochemical mechanisms driving the development of water in a natural and non-industrial setting. To understand the hydrogeochemistry of the region, several ionic and molar ratios, as well as Piper's trilinear diagram, are used. The chemical makeup of surface water and spring water is shown by triangular diagrams for measured anions and cations. Piper trilinear diagrams are used to characterize the hydrochemistry of water. $\text{Ca-HCO}_3^- > \text{Ca-Mg-HCO}_3^- > \text{Na-HCO}_3^- > \text{Ca-SO}_4^-$ were the five water types found by Piper diagram. The water types Ca-HCO_3^- , Ca-Mg-HCO_3^- , and Mg-HCO_3^- indicate a carbonate lithology as the host rock, whereas the water type Na-HCO_3 shows how water interacts with silicate lithologies in the region.

S. Li et al., 2009; S. Li & Zhang, 2008 conducted research at China's Upper Han River basin in order to quantify human influence and chemical weathering on dissolved loads. Collected water samples are tested for cations and anions by inductively coupled plasma and atomic emission, respectively. Anthropogenic interference and rock weathering both add solutes to rivers, and their relative contributions is calculated based on the concentration of dissolved anions and cations. The Han River Basin's waters are somewhat alkaline, and there is a significant correlation between electric conductivity, cations, and anions. $\text{Ca} > \text{Mg} > \text{Na} > \text{K}$ and $\text{HCO}_3^- > \text{SO}_4^{2-} > \text{Cl}^- > \text{NO}_3^- > \text{F}^-$ are the major ionic concentrations in the region. The chemical species of waters are discovered to arise from rock weathering and its minerals

in the drainage basin, the atmospheric deposition, and human inputs by analyzing different combinations of ions and their ratios. The weathering of carbonates and silicates dominates the chemistry of the river water in the area. Limestone, dolomite, and silicate rocks are three end-members that are distinguished by chemical weathering of minerals.

Khanoranga & Khalid, 2019 studied three areas in Balochistan, Pakistan, to assess the quality of groundwater that is used for irrigation and domestic use near brick kilns. A total of 22 physico-chemical characteristics were used to appraise the groundwater quality. The Piper Hill diagram is used in hydro-chemical analysis. The water quality index (WQI) is utilized to assess the water suitability for consumption. The salt absorption ratio (SAR), residual sodium carbonate (RSC), sodium percentage (Na%), and the permeability index were used to ascertain the groundwater suitability for irrigation cause. For geographic variability, source characterization, and dependency of numerous variables, multivariate statistics such as Principal component analysis (PCA), Cluster analysis (CA), and co-relation matrix were utilized. The examined region's geochemistry reveals a dominant pattern of principal cations and anions as $\text{Na}^+ > \text{Mg}^{+2} > \text{Ca}^{+2} > \text{K}^+$ and $\text{HCO}_3^- > \text{SO}_4^{-2} > \text{Cl}^- > \text{F}^-$. The Piper diagram reflects the geology by showing the hydrochemistry of the region as CaCl and NaCl water types. The groundwater quality in WQI is poor and unfit for drinking. Only with regard to SAR and PI was groundwater suitable for irrigation. The findings of multivariate statistics revealed that geological composition and anthropogenic activities in the region had a significant impact on groundwater.

Islam-ud-Din, Shah, M. T., & Khan, S. (2010) investigated how metals leaching from tropical soil in Bangladesh affects lake and reservoir water quality. They looked at metal release during weathering to see whether there were any geochemical controls

in place and if there were any negative consequences for Bangladesh's ecosystem. They observed that Al, Mg, Ca, Na, K, As, Ba, Cr, Ni, Pb, and Zn were usually higher in all surface water samples during the comparative investigation of four locations (Rajarampur, Shamta, Mainamoti, and Andulia in Bangladesh). According to the data, climatic conditions have a significant role in the process of degradation. Metal enrichment in lake and reservoir water is caused by metal ion solubility, organometallic complexes, and co-precipitation or co-existence with the colloidal clay fraction. Aluminum concentrations in all samples surpass WHO's drinking-water guidelines, while arsenic concentrations in two regions also considerably exceed WHO criteria. The high concentration of As suggest that the pollution of Arsenic in water systems of Bangladesh is not limited to groundwater.

Lake Baikal is a natural lake in southern Siberia, located between the Buryat Republic and the Irkutsk Oblast of Russia; Sinyukovich, 2003 studied its water quality and environmental elements. The total dissolved solids (TDS) discharge from the lake's major tributaries was studied, and an inverse connection was found between water flow and TDS in river water. The inverted connection may be attributed to the occurrence of hardly soluble gneisses, conglomerates, crystalline schist, and dolomite in the geological structure of their watersheds. The study found that the availability of river water has a key influence in controlling dissolved solids discharge, and that further research into this area will help improve our knowledge of how total dissolved solids discharge is formed in Lake Baikal.

3 STUDY AREA

Gilgit Baltistan, formerly known as Northern Pakistan, with a population of about 2 million is a remote mountainous region renowned as the "Roof of the World," covering 72,500 square kilometers. It is located between 35° 0' and 37° 0' N, and 72° 0' to 75° 0' E, with elevations ranging from 1500 to 8000 meters above sea level with a mean elevation of 4600m and is surrounded by high mountains. It is bordered on the north by China's Xinjiang region, on the south by Pakistan's Khyber Pakhtunkhwa province, on the east by Kashmir, and on the west by Afghanistan. Pakistan's Northern Areas are surrounded by three prominent mountain ranges: the Himalayas, Karakoram, and Hindukush. Mountain ranges consist of numerous gigantic and snowcapped peaks, such as the K-2 (8613 meters), Nanga Parbat (8126 meters). The glaciers Mashabrum, Siachen, Rakaposhi, Haramosh, and Passu are among the biggest in the world.

Pakistan is divided into two major sedimentary basins; Balochistan basin and Indus basin. There are two distinct regions within the Indus basin, Upper and lower Indus basin. Gilgit Baltistan lies in the upper Indus basin of Pakistan. The Indus Basin provides essential drainage for the northwest Himalayas and the Karakoram range, covering an area of roughly 863,508 km². The Indus river's major headwaters are in India and China. The Shingo, Shyok, Shigar, Astore, Hunza, Gilgit, and Kabul rivers are the sub basins of the upper Indus Basin (Abro et al., 2020). The sub-basins mostly rely on snow and glacier meltwater for their water needs (Amin et al., 2018). The main rivers flowing through the study area are Ghizer river, Gilgit river, Hunza River and Skardu river. Glacial fed channels along these rivers and its surrounding areas were selected to collect water samples for the laboratory analysis.

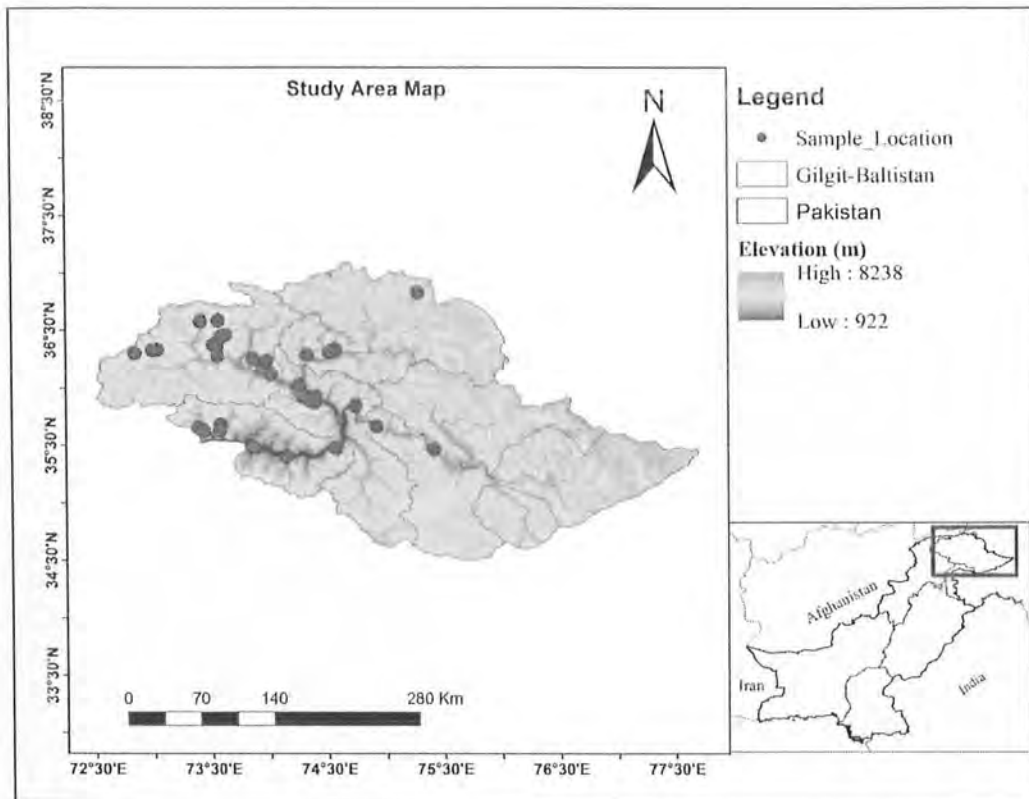


Fig 3. 1 Sampling Locations of the Study Area

3.1 GILGIT RIVER BASIN

The Gilgit river basin is situated in the Hindukush-Karakorum-Himalaya area, between 35°80'N and 36°91'N and 72°53'E and 74°70'E in latitude and longitude respectively, and drains south eastward into the Indus River. Because it is a glacierized basin, any changes in climate will have an influence on the frozen water resource, affecting the inflow to the Indus Basin irrigation system (Adnan, Nabi, Saleem Poomee, et al., 2017). Gilgit river is the major tributary which originates from the Shandoor lake Chitral Pakistan (Adnan, Nabi, Saleem Poomee, et al., 2017; Ahmed et al., 2021). The Gilgit River's main right bank tributary, Baha Lake, is located close by the Handrab and Langar rivers. From the left bank, tiny rivers like as the Phandar, Ishkoman and Yasin River flow into Gilgit river. Near Ghizer's Phandar Lake, the Phandar River merges into the Gilgit river. The Yasin River and Gilgit River meet at Gupis village. The Gilgit

river is fed by the glaciers of Karakoram and Hindu-kush mountains. The Gilgit River flows through Gilgit District from west to east and eventually empties into the Indus. The mean height of the basin is at 3997 m, and the drainage area is around 12,671 km² according to the Gilgit river gauging station. The area of the watershed over 5000 meters is mostly covered in permanent snow, and the glaciers are well preserved (Adnan, Nabi, Kang, et al., 2017). Volcanic, volcanic-sedimentary, sedimentary, metamorphic, and igneous rocks are the most common types of rock formations in the basin (Bhutani et al., 2009). Type of rocks in these exposed rock formations include siliciclastic, granite, basaltic, andesitic, rhyolitic, carbonates, gabbro, phyllite, greenschist, and so on. The high mountains of Gilgit Baltistan are permanently covered in snow, while the lowlands around the country's rivers and valleys are home to farms and forests.

3.2 CLIMATE OF THE AREA

Climate refers to the average weather conditions over a lengthy period of time in a particular area. Some scientists describe climate as the long-term average of a region's weather, often over the course of 30 years. It is one of the most essential factors of our physical environment, influencing not only human evolution but also their personalities, modes of living, cultural, and social traits. Human activities such as agriculture, population expansion, industrialization, and transportation, on the other hand, have an impact on the climate. The study of climatology is, in general, deeply entwined with the concerns of daily living (S. Khan et al., 2020). From summer to winter, the average yearly temperature of Gilgit-Baltistan is between 35°C and -20°C (N. Khan et al., 2019). From June to December, the average yearly humidity level ranges from 23 to 55 percent. The region's typical annual rainfall ranges from 200 to 250 millimeters (Faisal.N & A.Gaffar, 2012). Local thunderstorms have brought heavy precipitation to the Gilgit Baltistan area. There are four distinct rainy seasons in the

area, beginning with winter rains and continuing through pre-monsoon rains, monsoon rains, and post-monsoon rains. Winter, the beginning of the monsoon, and the monsoon are all wet periods in the province, whereas the end of the monsoon is the dry period. Latitude, altitude above sea level, rugged topography, continentality, snow cover, vegetation, and soil contents are all elements that influence the climate of Gilgit Baltistan province. Based on average annual temperatures, the Gilgit Baltistan area is divided into three distinct climatic zones: warm, cool, and cold. Summer in this area lasts for five months (May–October), whereas winter (November–April) is much shorter.

4 RESEARCH METHODOLOGY

4.1 FIELD WORK

The following approaches were used to collect water samples from high-altitude glacially-fed Nullahs/streams and springs that cross the main KKH in the research region (Ghizer, Gilgit, Nagar, Hunza).

4.1.1 Water Sampling

In order to assess the water quality, forty water samples were taken from glacier-fed streams and springs in the research region. The polyethylene bottles were cleaned with double-ionized water before to collecting the water sample. All water samples were collected according to APHA requirements. At each site, a single water sample is obtained. Approximately four to five water samples were obtained along the main stream from Hundrap hamlet Ghizer to Gilgit city in order to measure the turbidity levels of the river. During the sampling of climate, geology, land use, geogenic and anthropogenic activities, their geographical locations will be captured using a hand-held GPS device.

4.2 DETERMINATION OF PHYSICAL PARAMETERS

Among the physical characteristics that were measured in the field were temperature, electric conductivity (EC), pH, turbidity, and total dissolved salts (TDS). Before the in-situ measurements, the equipment was calibrated.

4.2.1 Determination of Temperature

One of the most important features that should be considered is the temperature of the aquatic environment since it controls practically all physical, chemical, and biological aspects. Saturation levels of gases and solids in water are controlled by the temperature. The temperature of the water is a crucial determinant of the species found

in streams and lakes. A thermometer was used to determine the temperature of water samples taken in the field.

4.2.2 Determination of pH

One of the most common tests in water chemistry is pH measurement. Acidity and alkalinity of any fluid is quantified on the pH scale. Field water samples were tested for acidity using a Hanna pH meter.

4.2.3 Determination of Electric conductivity

Conductivity is the capacity of a material to conduct an electric current. Because the charge on an ion in a solution promotes electric current conductance, conductivity is proportional to ion concentration in a solution. In the field, the electrical conductivity of water samples was determined in s/cm using a Lovibond sensing-direct conductivity meter.

4.2.4 Determination of turbidity

The turbidity of water causes light to be dispersed or absorbed rather than transmitted straight through the sample. Turbidity is caused by the size, shape, and refractive index of suspended particles rather than the concentration of the latter found in water samples. The turbidity of the collected water samples is measured in the units of NTU in the field by a conductivity meter.

4.2.5 Determination of Total Dissolved Solids (TDS)

Total dissolved solids in water are the residue left behind after evaporation of the water away at temperatures between 103 and 105 degrees Celsius. In a water body, total dissolved solids (TDS) are predominantly inorganic salts with a minute number of organic materials. Natural processes involving rock and soil contact are the primary contributors of TDS in water, with pollution having only a secondary role (Sinyukovich, 2003). TDS readings for water samples were determined in mg/L using

a Lovibond senso-direct meter in the field. Table 4.1 shows the field equipment used to measure the physical properties of water samples.

Table 4.1 List of Equipment Used in Field for the Measurement of Physio-Chemical Parameters

Instrument	Model no	Detection range	Measured Parameter
Turbidity meter	430-260	0-1000 NTU	Turbidity
Hanna pH meter	HI8424	-2 – 16 pH	pH
Lovibond Senso-direct	Con-200	0 – 200 μ s/cm 0 – 1999 mg/l	Electrical Conductivity Total Dissolved Solids

4.3 DETERMINATION OF CHEMICAL PARAMETERS

Lab tests are performed on the water samples once they have been collected. Major anions and cations concentrations are evaluated to assess water quality. Multiple laboratory techniques are used to determine the hardness of water samples and their concentrations of main cations (Ca^{2+} , Mg^{2+} , Na^{+2} , K^{+}) and anions (Cl^{-} , HCO_3^{-} , SO_4^{-2} , PO_4^{-2} , NO_3^{-}).

4.4 DETERMINATION OF ANIONS

4.4.1 Chloride (Cl^{-})

The concentration of chloride was studied in the lab using the argentometric titration technique. AgNO_3 0.014N is used as standard solution and K_2CrO_4 is used as an indicator. Each sample of water is analyzed by adding 2–3 drops of indicator to 10 ml of water in a beaker. Then it is titrated against the standard solution of AgNO_3 until the end point red brick color appears. The same procedure is repeated for the blank solution and the value of titrant consumed is recorded. Concentration of Cl^{-} is then calculated by using the formula:

$$Cl (mg/l) = \frac{(A-B) \times 35.45 \times 1000}{\text{Sample Volume in ml}}$$

Where,

A = reading of the specimen

B = blank-solution reading

N = 0.014

4.4.2 Sulfate (SO_4^{2-})

The Turbid metric spectrophotometric (model NV 202) method was used to determine sulphate. Conditioning reagent, Barium chloride solution, and Standard Sulfate solution are the chemicals utilized. In 100ml volumetric flasks, standard sulphate solutions of 5, 10, 20, 30, 40, and 50ml are made and diluted to the mark with DDW. Six separate beakers are used to transfer the liquids. In a flask, 100 ml of water is added with continual stirring, followed by 5 ml conditioning reagent and 5 ml BaCl_2 solution. As a blank sample, double deionized water is utilized. The Spectrophotometer wavelength is set at 420nm. Blank was used to set the absorbance value. The absorbance of the reagent blank is measured. The calibration curve of absorbance vs sulphate concentration in mg/l is plotted on an excel sheet in the last stage, and the sulphate concentration in the water samples is calculated.

4.4.3 Phosphate (PO_4^-)

The Spectrophotometric technique is used to calculate the phosphate concentrations in the water samples. Phosphate is measured using ammonium molybdate and stannous chloride as reagents. Using an Erlenmeyer flask, we collected a total of 26 ml of sample (2 ml of sample plus 24 ml of DW). Mix 1 milliliter of ammonium molybdate solution by swirling it around in the flask. We put in two drops of stannous chloride solution. There was a dash of ascorbic acid added and blended in. Phosphate was quickly identified thanks to the development of a blue hue in only five minutes. A spectrophotometer with a 650nm wavelength was used. For this experiment,

the zero absorbance was determined by using a blank solution. The absorbance of the sample was determined by analyzing its color at 650 nm on the spectrophotometer. Standard curve analysis was used to ascertain sample concentration.

4.4.4 Nitrate (NO_3^-)

Both freshwater and sewage contain nitrates as a natural occurrence. Nitrate poisoning of water sources is caused by decomposition of natural vegetation, application of agrochemicals, and oxidation of nitrogenous compounds in sewage effluents and industrial wastes. It is possible to determine the amount of NO_3^- in water samples by a colorimetric examination in the lab. Bruciline-sulfanilic acid solution, sulfuric acid solution, sodium chloride stock nitrate solution, and anhydrous KNO_3 were used as reagents. 5mL, 10mL, 15mL, and 20mL standard nitrate solutions are made. Each flask is filled with 2 mL NaCl and 10 mL 4:1 H_2SO_4 solution, which is thoroughly mixed. Each flask receives 0.5mL of Bruciline acid reagent. The spectrophotometer was set to zero at 410nm after preparing a blank with distilled water. Now take a note of the absorbance values of each of the standard solutions. The absorbance of the samples was measured after 10ml of sample was added to reagents and the yellow color developed. Using the standard curve, the concentration of the sample was determined.

4.4.5 Carbonate (CO_3^{2-}) and Bicarbonate (HCO_3^-)

Carbonates and bicarbonates were measured using the titration technique with 0.1N hydrochloric acid in all water samples. As markers for carbonates and bicarbonates, phenolphthalein and methyl orange were utilized. To do the titration, we put 25 ml of water sample into a 250 ml flask and added 3 drops of phenolphthalein. There was no color change, indicating that there was no carbonate present in the water samples. 2-3 drops methyl orange were added to the same amount of water sample for

HCO₃ determination and light orange color develops. Sample is titrated against 0.1N HCl from the burette, until the light orange color vanished. The amount of acid used was reported in milligrams per liter in terms of CaCO₃ using the formula below.

$$\text{mg/l of CaCO}_3 = \frac{(\text{Volume of titrant consumed} \times 0.1) \times 50,000}{\text{Volume of Sample}}$$

4.5 DETERMINATION OF CATIONS

4.5.1 Sodium and Potassium

Sodium and potassium are important elements in humans. Despite this, they are seldom, if ever, found in drinking water in concentrations that might be detrimental to healthy individuals. Sodium and potassium levels in the water samples were calculated using the flame photometric method. Na and K stock standards (1000mg/L) were prepared by dissolving 2.542g NaCl and 1.91g KCl in deionized water, and then filling a volumetric flask with 1000ml of the resulting solution. Assay standards of 5, 10, and 15 ppm were prepared using this stock solution. The flame photometer wavelength is set at 589nm for Na⁺ and 766nm for K⁺. Blank was used to set the absorbance value. Now take 50ml of samples in a flask and record the readings. Plot a calibration curve for the result values of standard solutions and determine the concentration of Na⁺ and K⁺ for the water samples from the plot. After every ten samples, blank and working standards were run to ensure instrument calibration and analysis accuracy.

4.5.2 Calcium and Magnesium

Titrimetric analysis of ethylene-diamine-tetra-acetic acid (EDTA) allows for the measurement of Ca²⁺ and Mg²⁺ concentrations. EDTA solution of 0.1M, ammonia buffer solution and NH₄Cl are used as reagents. To make the solutions, fill a flask halfway with distilled water and add 3.7g EDTA solution with a molarity of 0.1. In a separate flask, make a 300ml ammonia buffer solution, add 21g of NH₄Cl, and top up to 500ml with distilled water. As for indicators, Eriochrome Black T acid (EBITA) for

magnesium and Murexide for calcium are utilized. The concentration of magnesium is measured by adding 6ml of ammonia buffer solution to 10ml of water in a flask. When a few drops of the EBITA indicator are applied, the color changes to purple. The pigment is then titrated against the burette's EDTA solution until it turns blue. Take note of the titrant consumption data from the burette. The same approach is used to determine Ca using Murexide as an indicator. The initial and final colors for calcium are orange and light pink, respectively. Ca^{+2} and Mg^{+2} concentrations are calculated by plugging values into the formula below.

$$Ca^{+2} \text{ or } Mg^{+2} = \frac{(A-B) \times D \times 1000}{\text{Volume of Sample}}$$

Where,

A = measure of sample's titrant used in milliliters

B = amount of titrant needed for blank

D = 0.1M

4.5.3 Hardness

Hardness in water is caused by a wide range of polyvalent metallic ions, most notably calcium and magnesium cations. Measured most often in milligrams of calcium carbonate per liter. Hardness for the current study is determined by using the formula...

$$\text{Hardness} = (Ca + 2) \frac{(MwCaCO_3)}{(MwCa+2)} + (Mg + 2) \frac{(MwCaCO_3)}{(Mwmg+2)}$$

Where, Mw is the molecular weight

The summary of the testing methods used to determine the concentration of cations and anions is shown in the table 4.2.

Table 4.2 List of Laboratory Methods Used in Measurement of Anions and Cations

Parameter	Unit	Test Methods
Chloride (Cl ⁻)	mg/L	Argentometric Titration
Sulfate (SO ₄ ⁻²)	mg/L	Spectrophotometrically
Phosphate (PO ₄ ⁻²)	mg/L	Spectrophotometrically
Nitrate (NO ₃ ⁻²)	mg/L	Spectrophotometrically
Bicarbonate (HCO ₃ ⁻²)	mg/L	Titration method
Sodium (Na ⁺)	mg/L	Flame Photometric
Potassium (K ⁺)	mg/L	Flame Photometric
Calcium (Ca ⁺²)	mg/L	EDTA Titrimetric
Magnesium (Mg ⁺²)	mg/L	EDTA Titrimetric

4.6 DETERMINATION OF HEAVY METALS

For the purpose of this investigation, the following heavy metals were chosen: manganese (Mn), iron (Fe), zinc (Zn), chromium (Cr), lead (Pb), cadmium (Cd), copper (Cu), mercury (Hg), and arsenic (As). To assess their concentration in collected water samples, table 4.3 details some of the most often used methods.

Table 4.3 List of Laboratory Methods Utilize for the Measurement of Concentration of Heavy Metals for Collected Water Samples

Heavy Metals	Units	Instrument & Model No	Test Methods
Chromium (Cr)	µg/L	AAS Perkins Elmer A-Analyst 800	Spectrophotometric method
Cadmium (Cd)	µg/L	SHIMADZU UV Spectrophotometer (FWTL/1800)	Atomic Absorption Spectrophotometric
Lead (Pb)	µg/L	AAS Perkins Elmer A-Analyst 800	Atomic Absorption Spectrophotometric
Zinc (Zn)	µg/L	UNICAM Flame AAS (FWTL/013)	Atomic Absorption Spectrophotometric
Iron (Fe)	µg/L	SHIMADZU UV Spectrophotometer (FWTL/1800)	Spectrophotometric method
Copper (Cu)	µg/L	UNICAM Flame AAS (FWTL/013)	Atomic Absorption Spectrophotometric
Mercury (Hg)	µg/L	SHIMADZU UV Spectrophotometer (FWTL/1800)	Spectrophotometric method
Manganese (Mn)	µg/L	SHIMADZU UV Spectrophotometer (FWTL/1800)	Spectrophotometric method
Arsenic (As)	µg/L	Merck Arsenic Test Kit 1179170001	Colorimetric Arsenic test Strips

4.7 ANALYSIS AND EVALUATION

There are two basic components of water sample analysis and assessment used to determine the quality of the area's surface water i.e., is 1) Hydro-geochemical and Hydro-geostatistical analysis and 2) Machine learning methods for predicting water quality classes and their performance comparison. Thirteen physic-chemical parameters were evaluated, including pH, Turbidity, Electric Conductivity (EC), Total Dissolved Solids (TDS), Calcium (Ca^{+2}), Magnesium (Mg^{+2}), Sodium (Na^{+}), Potassium (K^{+}), Chloride (Cl^{-}), Sulfate (SO_4^{-2}), Phosphate (PO_4^{-2}), Nitrate (NO_3^{-2}), and Total Hardness. The evaluation takes into account the following heavy metals: chromium

(Cr), zinc (Zn), lead (Pb), iron (Fe), copper (Cu), cadmium (Cd), mercury (Hg), manganese (Mn), and arsenic (As).

4.7.1 Hydro-Geochemical Analysis

Hydro-geochemical analysis is performed to assess and categorize surface water quality. The assessment was conducted through the classification of the water quality using the water quality index (WQI). Water quality is measured on the Water Quality Index (WQI), which takes into account a wide range of factors. It illustrates how various characteristics might affect the overall quality of drinking water (Khanoranga & Khalid, 2019). Hydro-chemical and hydro-geochemical plots i.e., Piper plot and Gibbs plot respectively are used to learn more about the geochemical mechanisms at play in regulating water chemistry and the larger picture of water chemistry. The contamination status of water samples is also determined by the heavy metal pollution index (HPI). The combined impact of each heavy metal with regards to the quality of the water supply and the suitability for human consumption were assessed using the pollution index (Appiah-Opong et al., 2021). Data calculation and graphical representations were done using Microsoft Excel (Version 2019). Grapher software (Version 2016) is used to create the Piper plot.

5 RESULTS AND DISCUSSIONS

5.1 WATER CHEMISTRY

Pure water molecule is chemically made up of two hydrogens and one oxygen atom. Such a molecule is not present in the natural world, neither in polar ice caps, clouds, rain, falling snow, or glacial stream and lakes. In a laboratory, it is possible to produce pure water, but it requires tremendous effort. Different types of water bodies have different water chemistry (in air, snow, rivers, lakes and oceans). Fresh water flows on the surface of the earth as rain and snow throughout the hydrological cycle of water. As it comes from high altitudes, it incorporates different substances from the nearby catchments, which results in its contamination. Water receives and retains foreign objects in a variety of ways, including:

1. Since water dissolves both salts and inorganic minerals, which often include negative ions and positive ions, as well as organic molecules like organometallic complexes, it is an excellent solvent in nature.
2. If the insoluble particles are tiny enough, they may settle so gradually that they practically never leave the water.
3. The soluble substances interact with insoluble particles and make them part of the solution.
4. Contaminants in the form of oil spills and other waste materials that float on the water's surface.

The interaction of the water with the soluble minerals of the bedrock in their courses, soil, and vegetation in the catchments are the numerous developments that affect the chemistry of the glacial-fed streams. Water chemistry is influenced by the mineralogy of bedrock because of the dissolution of minerals and solutes during weathering and erosion (Psenner & Catalan, 1994). Vegetation has an effect on

precipitation, transportation, and the deposition of ions and nutrients, even if a cation exchange complex may be provided by the soil (Stumm and Morgan, 1996). Anywhere, human activity may worsen or enhance the quantity and quality of water. It should be our mission as human beings to seek for solutions to preserve pure water for the sake of generations to come (Soomro, 2004).

5.2 WATER CHEMISTRY OF THE UNDER-STUDY REGION

The physiochemical properties of a body of water define its quality and characteristics. These parameters allow us to categorize where the water is healthy or contaminated for the human use. Samples of water from 40 representative streams in the Gilgit river basin, all of which are fed by glaciers at high elevated positions, were studied for their varied physiochemical features in order to determine the possibility of geogenic and anthropogenic pollution. The estimation of the physiochemical parameters in the water samples was done using standard test protocols. The physiochemical parameters include EC, pH, turbidity, hardness, TDS, Ca^{+2} , Mg^{+2} , K^{+} , Na^{+2} , SO_4^{2-} , NO_3^{-} , HCO_3^{-} , PO_4^{-} , Cr, Pb, Cd, Zn, Fe, Hg, Mn, and As. The World Health Organization's (WHO, 2022) recommendations were then compared to all measured values for all physiochemical parameters. The details of their findings are provided below.

5.3 ION CHARGE BALANCE ERROR

The electrical neutrality of an aqueous solution is a key characteristic. Since there must be an equal number of equivalents for positive and negative elements, the overall number of equivalents for each must be equal.

$$\text{Charge Balance} = \sum \text{cations} = \sum \text{anions}$$

A cation-anion balance will never be 100% accurate since it is almost difficult to evaluate each and every ion in a body of water. It is typically not necessary either. Nearly often, the ion charge balance in ground or surface water is more than 90%. To

assess the precision of the laboratory findings for the investigation of water quality, ion charge balance is utilized. Ion charge balance error (ICBE) should ideally be zero, however due to mistakes in the sampling process, instrument error, usage of unfiltered samples, change in circumstances, etc., it cannot have a value of zero. For analyses of water quality, an error value of up to $\pm 10\%$ is fine (Domenico & Schwartz, 1998). Mathematically, it may be expressed as:

$$ICBE (\%) = \frac{\sum cations - \sum anions}{\sum cations + \sum anions} \times 100 \quad (1)$$

A positive or negative ICBE is possible. An elevated concentration of cations in comparison to anions is indicated by a positive ICBE. A negative ICBE, on the other hand, signifies a greater abundance of anions. In the present investigation, only three of the forty samples display a negative charge balance, with the remaining thirty-seven samples displaying a positive charge balance. In the equation above, the ionic concentrations were measured in meq/L (milliequivalent per liter). The mean ICBE value for the current research was determined to be 6.58% with a standard deviation of 4.54%.

5.4 CHARACTERIZATION OF INDIVIDUAL HYDRO-GEOCHEMICAL PARAMETERS

For both drinking and other uses, it is crucial to be able to tell the difference between the quality of water that comes from the surface and that which comes from deep down. Analytical results of the physicochemical parameters which includes pH, turbidity, EC, TDS, hardness Na^{+2} , Ca^{+2} , Mg^{+2} , K^{+} , SO_4^{2-} , NO_3^{-} , Cl^{-} , HCO_3^{-} , PO_4^{-} , Cr, Pb, Cd, Zn, Fe, Hg, Mn, and As for the current study is presented in table 5.1. All the quality parameters are then compared with the recommended guidelines given by

World Health Organization (WHO, 2022) presented in Fig (5.1, 5.2, 5.3, 5.4, 5.6, 5.7, 5.8, 5.9, 5.10, 5.11, 5.12, 5.13, 5.14, and 5.15). The different variables, including the mean, minimum, maximum, standard deviation, and concentrations of physicochemical variables include pH, total dissolved salts (TDS), total hardness (TH), electrical conductivity (EC), heavy metals, main anions, and cations are given in (table 5.1). In the sections that follow, a brief discussion of all of these physicochemical criteria and their comparison with WHO guidelines will be provided.

5.4.1 pH

The pH scale is used to express how acidic or basic a given aqueous solution is. Acidic liquids have lower pH values than basic or alkaline solutions. According to the analytical findings of the samples taken in the research region, 95% of the samples are alkaline (pH more than 7) while the remaining are acidic (Fig 5.1). The pH values of the gathered samples vary between (6.8-8.8) with an average of 7.88. It is determined that water samples from the stations ST-15, ST-35, and ST-36 are strongly alkaline (pH>8.5), exceeding the WHO permissible limits which shows that carbonate-dominated lithologies in the area may have an effect on the pH of fluids, which is a recognized factor in many processes (Dinka et al., 2015; Laar et al., 2011).

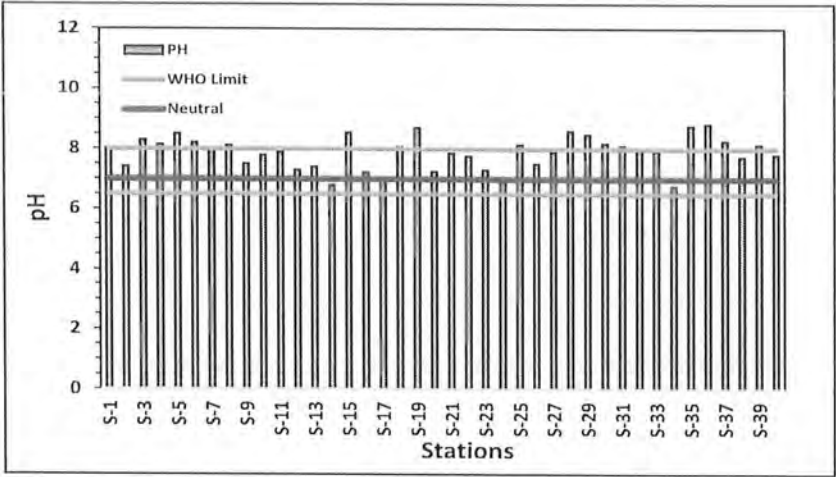


Fig 5. 1 Graph of pH for the Monitored Values of Physiochemical Parameters and Their Comparison with WHO limits

5.4.2 Turbidity

The turbidity of water is a measurement of the cloudiness of the water, which is caused by suspended large-sized solid particles as well as inorganic, organic, and microbiological species. Amongst the collected samples the turbidity values of seventeen samples were found high (Fig 5.2, table 5.1) above the permissible range (5 NTU) recommend by (WHO, 2022). The high values of turbidity are recorded because water samples were collected during the monsoon days and the waters of glacial fed streams get turbid due to flooding situations. The turbidity values of remaining water samples monitored within the permissible limits. Overall, the turbidity values amongst all the samples ranged between 1.1-126 with an average value of 17.38.

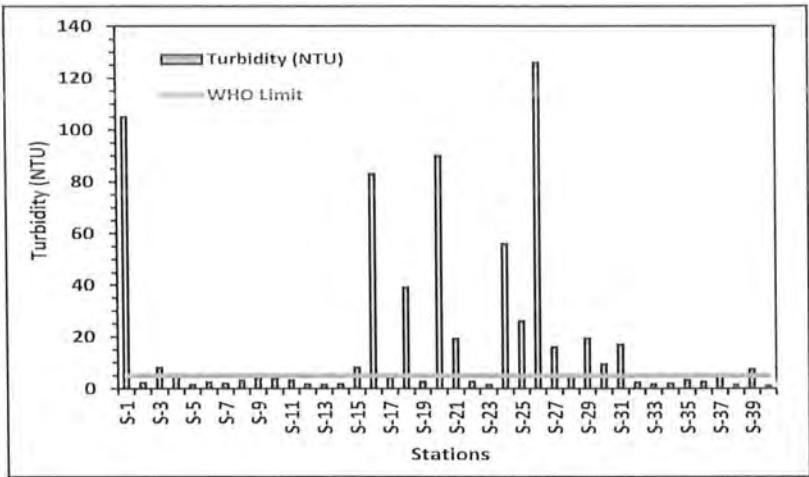


Fig 5. 2 Graph of Turbidity for the Monitored Values of Physiochemical Parameters and Their Comparison with WHO limits

5.4.3 Total Dissolved Solid (TDS)

The entire concentration of dissolved materials in water is expressed as total dissolved solids. TDS is mostly composed of inorganic salts, with a trace quantity of organic material. Inorganic salts that are frequently found in water include the cations potassium, calcium, magnesium, and sodium as well as the anions carbonates, nitrates, bicarbonates, chlorides, and sulphates. TDS values of the water samples ranged from 33 mg/l-389 mg/l with the mean value of 102.33 mg/L (table 5.1). All of the monitored values of TDS were found in the acceptable limits suggested by World Health Organization (Fig 5.3). Additionally, a recent research has also showed that the snow melting water of the region has a low TDS content. (Ahmed et al., 2021).

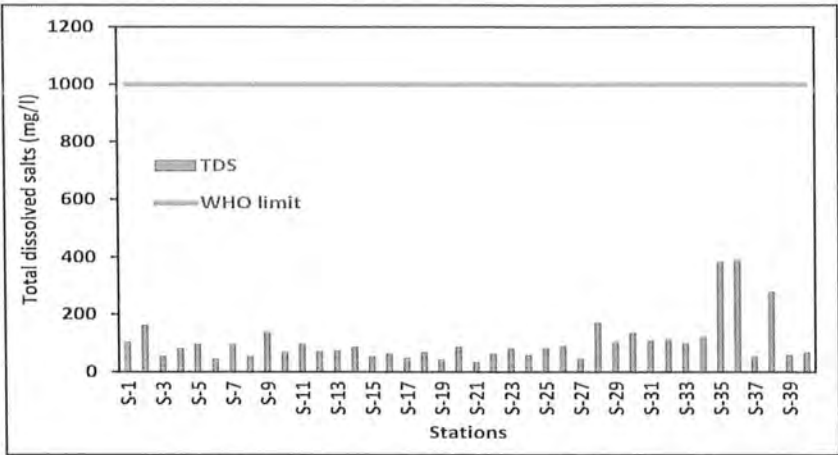


Fig 5. 3 Graph of TDS for the Monitored Values of Physiochemical Parameters and Their Comparison with WHO limits

5.4.4 Electric Conductivity

The capacity of a substance to carry electric current is measured by its electric conductivity. The conductivity will be better if there are more salts dissolved in the water. Total dissolved solids (TDS), often known as the total concentration of dissolved and particle solids in a water body, may be calculated using conductivity data. Micro-Siemens (μS) units are used to express the conductivity of water (Sinyukovich, 2003). However, EC values of the glacial waters of the region shows a wide variation 126.50 $\mu\text{S}/\text{cm}$ (table 5.1) ranging between 60 $\mu\text{S}/\text{cm}$ and 630 $\mu\text{S}/\text{cm}$ with an average of 160.80 $\mu\text{S}/\text{cm}$. All of the monitored values of EC were found within the permissible limits as illustrated in (Fig 5.4).

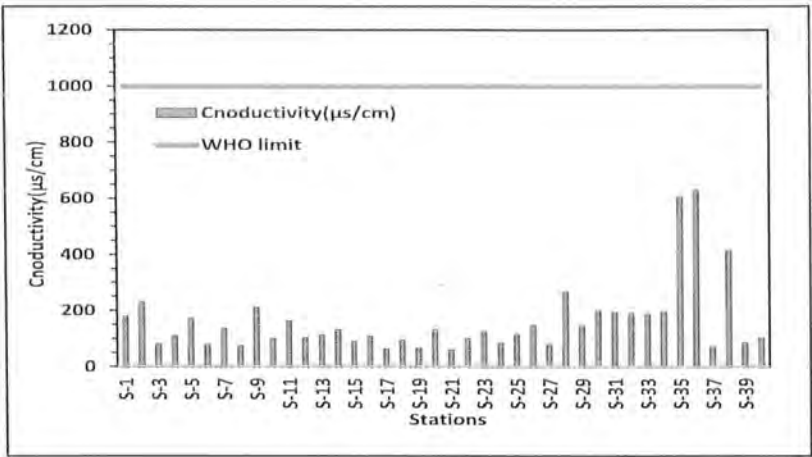


Fig 5. 4 Graph of Conductivity for the Monitored Values of Physiochemical Parameters and Their Comparison with WHO limits

5.4.5 Total Hardness

The total number of bivalent metallic ions in a body of water is considered to be its hardness. Calcium and magnesium are the primary sources of water hardness. In addition to manganese (Mn^{2+}), iron (Fe^{2+}), zinc (Zn^{2+}), strontium (Sr^{2+}), and other ions, hardness of the water is also influenced by these elements. Though often far lower than the levels of calcium and magnesium, their concentrations are nonetheless noticeable. Commonly hardness is expressed in parts per million (ppm) or parts per billion (ppb). Fig 5.5, and table 5.1 shows the hardness values for all observed samples. The results were within the allowable range of 0-500 mg/l that varied from 188mg/l to 480 mg/l with mean value of 298 mg/l. The majority of these samples are classified as hard or very hard waters. The major cause of the high total hardness is the excessive number of cations and anions that have been dissolved in water as a result of prolonged contact with rocks until the water reaches lower altitudes.

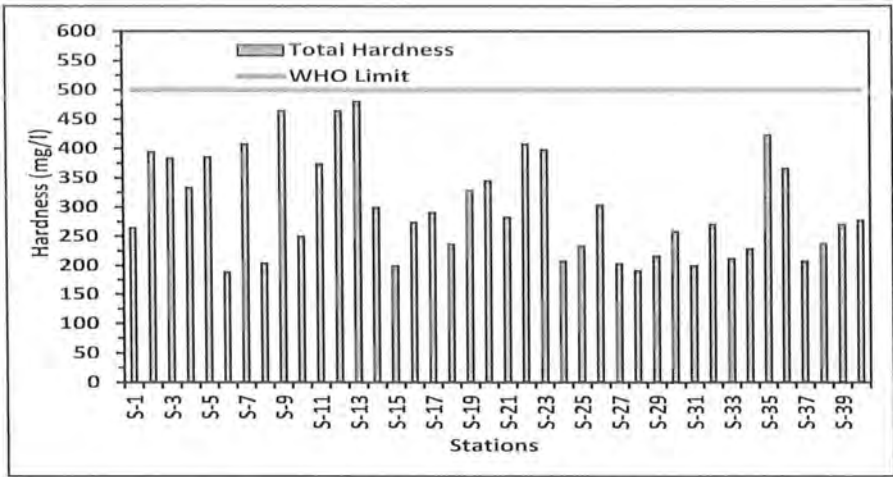


Fig 5. 5 Graphs of Hardness for the Monitored Values of Physiochemical Parameters in Contrast to the WHO's recommended levels

5.5 CATIONS

5.5.1 Sodium (Na^{2+})

In the earth's crust, sodium makes up around 2.6% by weight. Due to its extreme reactivity, this metal only ever appears in nature as a combination and never as a free element. Numerous minerals contain sodium, including zeolite, amphibole, cryolite, and common salt (Islam-ud-Din, Shah, M. T., & Khan, S. (2010)). Monitored values of sodium concentrations of the collected water samples are shown in the table 5.1 and graphically compared with World health Organization permissible limits in Fig 5.6. As per (WHO, 2022) the acceptable limits for the concentration of Na^{2+} is 100 mg/l and 95% of the sodium levels in the research area's samples are well within acceptable ranges. The remaining two samples exceeds the WHO prescribed limits. Overall, the sodium concentrations ranges from 5.5 mg/l to 125 mg/l with a mean value of 22 mg/l (table 5.1). The formation of rock salts, carbonate rock weathering, and the displacement of Na^{2+} ions from a complex of absorbed rocks and soils by Ca^{2+} and Mg^{2+} are possible sources of Na^{2+} ions (Dinka et al., 2015).

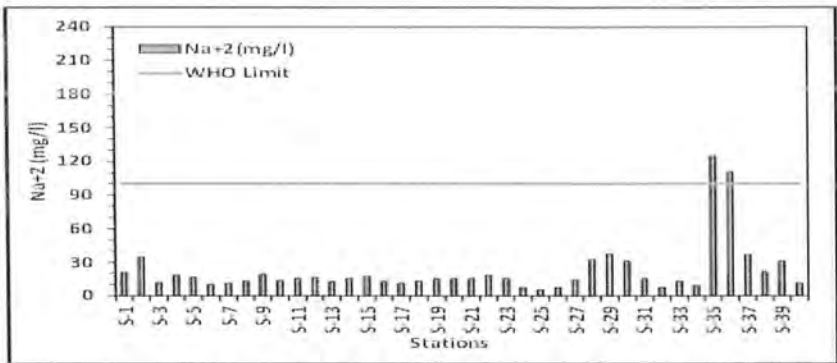


Fig 5. 6 Graph of Sodium (Na^{2+}) for the Monitored Values of Physiochemical Parameters in Contrast to the WHO's recommended levels

5.5.2 Potassium (K^{+})

Potassium is a silver-white metal that only occurs in small amounts in water due to its poor solubility in it. In table 5.1, we can see the sodium levels in the water of glacially fed streams in the studied regions as well as visually represented and compared with WHO standards in Fig 5.7. The monitored values of potassium were in the range of 5.7 mg/l to 38.7 mg/l with an average value of 13.77 mg/l. The WHO permissible limit for sodium concentration in water is 100 mg/l and concentration of all the tested samples were found within the limits indicating suitable for human consumption and irrigation use. The orthoclase feldspar, microcline, and biotite minerals found in the local granites are the source of potassium in the surface water (Adimalla, 2019; Trauth et al., 1997).

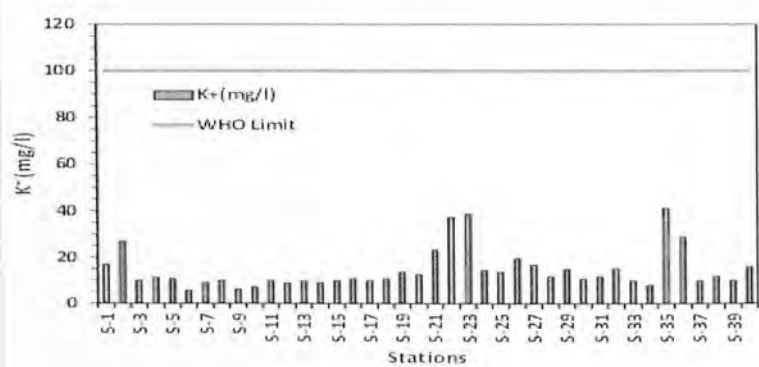


Fig 5. 7 Graph of Potassium (K^{+}) for the Monitored Values of Physiochemical Parameters in Contrast to the WHO's recommended levels

5.5.3 Calcium (Ca²⁺)

The regular development and maintenance of bones depend on calcium, which is regarded as a significant component of mineralized tissues in the human body. Water contains calcium in the form of calcium salts (CaCO₃ or CaCl₂). In the granitic terrain, calcium is obtained from feldspar, pyroxene, and amphibole minerals as well as from auxiliary minerals like apatite and fluorite (Adimalla, 2019; Dinka et al., 2015). The observed scores of the concentration of Calcium for the current investigation vary between 44 mg/l to 103 mg/l with mean value of 72.83 (table 5.1). The maximum threshold limit for calcium set by (WHO, 2022) is 300 mg/l and Calcium levels were all within the safe range for the samples that were examined (Fig 5.8) indicating suitable for drinking and other uses.

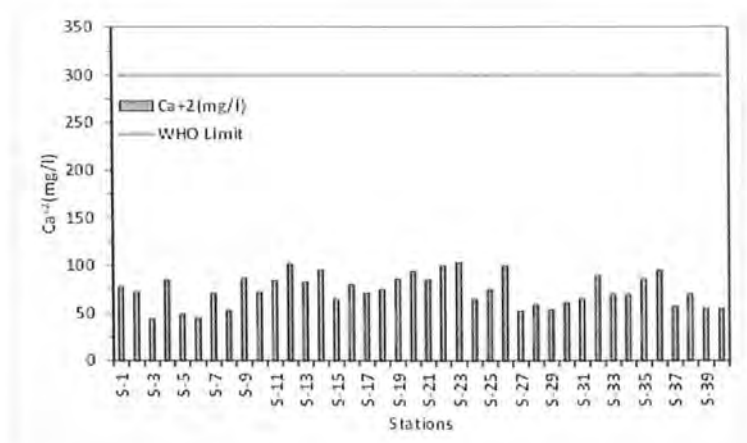


Fig 5. 8 Graph of Calcium (Ca²⁺) for the Monitored Values of Physiochemical Parameters in Contrast to the WHO's recommended levels

5.5.4 Magnesium (Mg²⁺)

Magnesium is present in several minerals, the most popular of which are magnetite and dolomite. Magnesium is also incorporated into water bodies by a variety of processes, such as weathering mafic and ultramafic rocks (Islam-ud-Din, Shah, M.

T., & Khan, S. (2010)). Concentrations of magnesium in collected water samples of the region are shown in table 5.1 and graphically presented and analyzed with the WHO standards in Fig 5.9. Its concentration found between 7 mg/l to 27 mg/l with an average value of 12.70 mg/l (table 5.1). In all of the representative samples the monitored values are found within the permissible limits. The measured result at ST-12 is 27 mg/l, which is quite near to the upper threshold level of 30 mg/l. The effect of ferromagnesian minerals found in the local rocks is responsible for this greater concentration of magnesium.

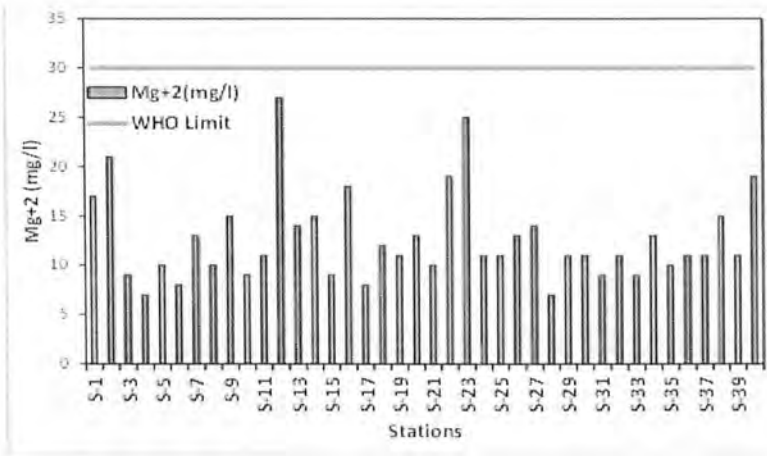


Fig 5. 9 Graph of Magnesium (Mg²⁺) for the Monitored Values of Physiochemical Parameters in Contrast to the WHO's recommended levels

5.6 ANIONS

5.6.1 Chloride (Cl⁻)

One of the main anions in water is chloride (Cl⁻), which is often coupled with calcium, magnesium, or sodium to produce soluble salts. Surface and groundwater chloride can come from both natural and anthropogenic sources (A. K. Tiwari & Singh, 2014). Monitored values of chloride for the collected water samples are presented in the table 5.1 and graphically compared with World health Organization permissible

limits in Fig 5.10. Throughout the study area, the Cl^- concentration in all samples of surface water was much below the acceptable threshold level, which is 250 mg/l for portable water, suggesting that the water is safe to consume and other applications. Overall, the chloride concentrations ranges from 39 mg/l to 106 mg/l with an average of 68.58 mg/l (table 5.1).

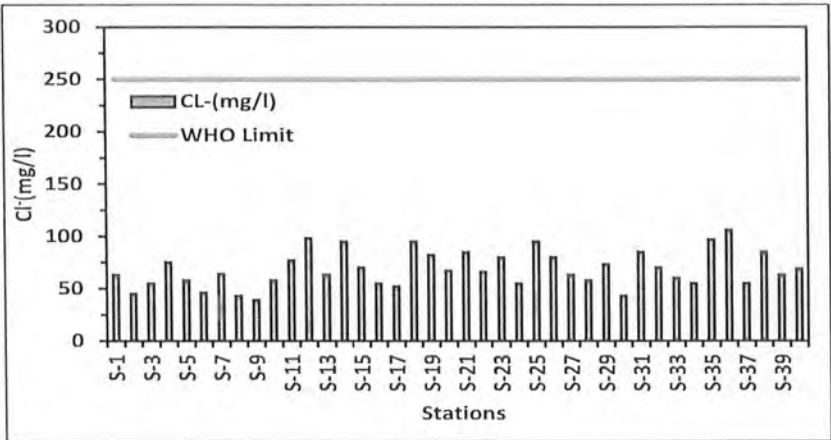


Fig 5. 10 Graph of Chloride (Cl^-) for the Monitored Values of Physiochemical Parameters in Contrast to the WHO's recommended levels

Table 5.1 Values of Physiochemical Parameters in Water Samples, Compared to Standard Acceptable Ranges

Parameters	N	Min	Max	Mean	St.dev	Variance	WHO Limit	ICBE Limit
Conductivity($\mu\text{S/cm}$)	40	60.0	633.00	160.80	126.5	16001.86	1000	-
Turbidity (NTU)	40	1.1	126.00	17.38	30.77	946.62	5	-
pH	40	6.8	8.83	7.88	0.54	0.29	6.5-8.5	-
TDS (mg/l)	40	33.0	389.00	102.33	79.49	6319.10	1000	-
Hardness (mg/l)	40	188.7	480.60	298.79	86.59	7497.79	500	-
Ca^{+2} (mg/l)	40	44.0	103.00	72.83	16.47	271.33	300	-
Na^{+2} (mg/l)	40	5.4	125.00	22.05	23.81	566.71	100	-
Mg^{+2} (mg/l)	40	7.0	27.00	12.70	4.55	20.68	30	-
K^{+2} (mg/l)	40	5.7	38.71	13.77	7.40	54.79	100	-
Cl^- (mg/l)	40	39.0	106.00	68.58	17.22	296.51	250	-
HCO_3^- (mg/l)	40	87.0	310.00	164.48	53.88	2903.23	500	-
NO_3^- (mg/l)	40	0.0	3.40	0.87	1.00	1.01	50	-
SO_4^{2-} (mg/l)	40	0.0	95.57	22.10	29.32	859.44	250	-
PO_4^{2-} (mg/l)	40	0.0	11.49	4.74	3.71	13.79	10	-
Cr (mg/l)	40	0.0	0.00	0.00	0.00	0.00	0.05	-
Pb (mg/l)	40	0.0	0.02	0.01	0.00	0.00	0.01	-
Cd (mg/l)	40	0.0	0.01	0.00	0.00	0.00	0.005	-
Cu (mg/l)	40	0.0	1.38	0.29	0.35	0.12	2	-
Zn (mg/l)	40	0.0	1.90	0.30	0.32	0.10	3	-
Fe (mg/l)	40	0.0	0.18	0.05	0.05	0.00	0.3	-
Hg (mg/l)	40	0.0	0.00	0.00	0.00	0.00	0.5	-
Mn (mg/l)	40	0.0	0.09	0.02	0.02	0.00	0.006	-
As (mg/l)	40	0.0	0.01	0.00	0.00	0.00	0.01	-
ICBE (%)	40	-9.4	9.84	6.58	4.53	20.57	-	$\pm 10\%$

5.6.2 Bicarbonate (HCO_3^-)

Water gains alkalinity, or the capacity to counteract acidity, from carbonates and bicarbonates. The carbonate, bicarbonate, and hydroxyl ions are responsible for alkalinity. Soft waters are often more acidic than hard waters, although the presence of carbonate and bicarbonate ions serves to buffer the system (Nollet & Gelder, 2000). The table 5.1 does not include CO_3 ions because their concentration is much lower than that of HCO_3 ions in the research region. The breakdown of carbonate rocks, such as limestone, dolomite, and magnesite, produces CO_3 and HCO_3 ions, which precipitate as CO_2 (Nikanorov and Brazhnikova, 2012). HCO_3 ions are also produced during the dissolution of carbonic acid H_2CO_3 (Ramesh and Jagadeeswari, 2012). HCO_3 ions are the dominant ions amongst anions. Monitored values of sodium concentrations of the collected water samples are presented in the table 5.1 and graphically compared with World health Organization permissible limits in Fig 5.11. As per (WHO, 2022) the acceptable limits for the concentration of HCO_3 is 500 mg/l and the bicarbonate levels in all the samples collected from the study region are well within acceptable ranges. Overall, the HCO_3 concentrations ranges from 87 mg/l to 310 mg/l with a mean value of 164 mg/l (table 5.1).

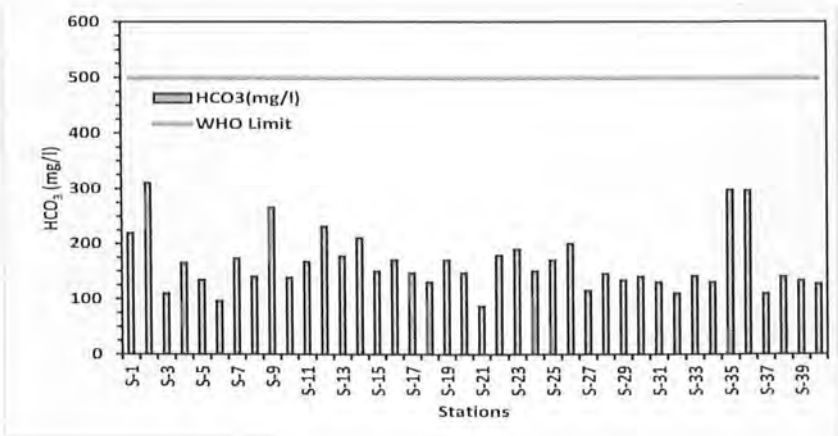


Fig 5. 11 Graph of Bicarbonate (HCO_3^-) for the Monitored Values of Physiochemical Parameters in Contrast to the WHO's recommended levels

5.6.3 Nitrate (NO_3^-)

Nitrate is a frequent food component, with vegetables often making up the majority of a person's daily diet intake. As a result of the excessive use of fertilizer in farmlands, nitrates are mostly released into the water from various agricultural operations (Towfiqul Islam et al., 2017). For the current region, (Fig 5.12, table 5.1) Out of 40 surface water samples, 14 samples had NO_3^- concentrations below the detectable limit, while the other samples have measured values that are significantly low compared to the permissible limit. These results may be attributed to the fact that the samples come from glacier-fed channels located at high elevations, where the dissolution of salts from glacial deposits might be a source of NO_3^- , and there were no or little up agricultural activities in the upstream (Ahmed et al., 2021; Nakhaei et al., 2015). Debernardi et al. (2008) examined the nitrate levels in groundwater and discovered that fertilizers were the main cause of the high NO_3^- levels. The overall concentration values of NO_3^- for the region of study ranges from 0-3.40 mg/l with an average of 0.87 mg/l (table 5.1). No probable NO_3^- contamination sources were discovered near the proposed water supplies.

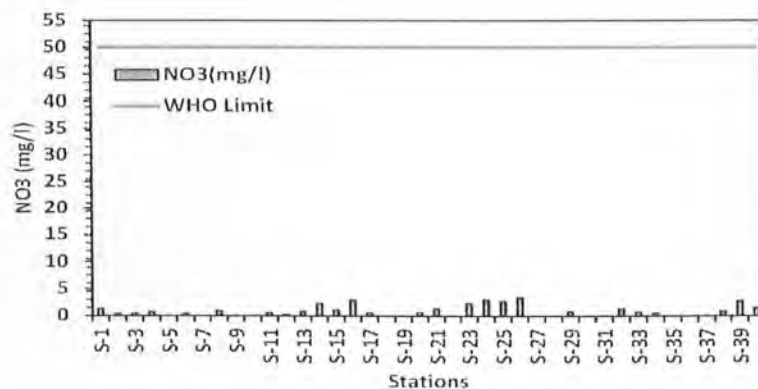


Fig 5. 12 Graph of Nitrate (NO_3^-) for the Monitored Values of Physiochemical Parameters in Contrast to the WHO's recommended levels

5.6.4 Sulfate (SO_4^{2-})

Sulfur and oxygen combine to make sulphate, which is a naturally occurring chemical. Minerals of varying types from different groups of elements, such as sodium, calcium, potassium, etc., were created by sulphate in soil. Water contains sulphates because leached magnesium, sodium, and potassium salts dissolve in water, but calcium and barium sulphate salts do not dissolve easily in water (Islam-ud-Din, Shah, M. T., & Khan, S. (2010)). The primary natural sources of SO_4 include biological reactions, weathering of sulfur-containing minerals such halite, gypsum, pyrite, and related mineral salts.

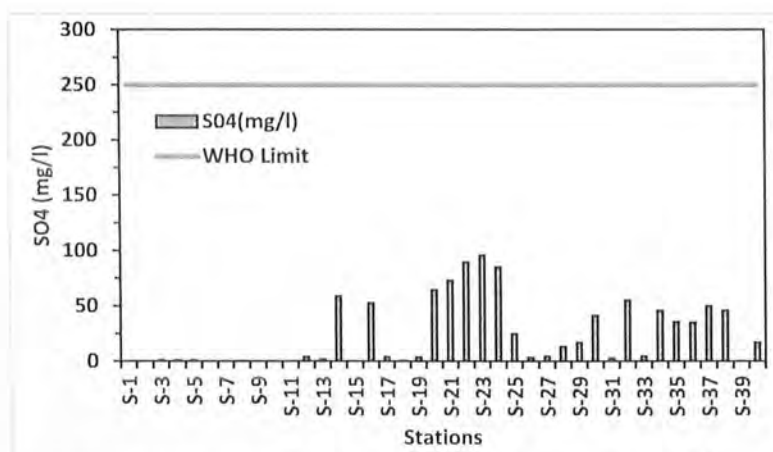


Fig 5. 13 Graph of Sulfate (SO_4^{2-}) for the Monitored Values of Physiochemical Parameters in Contrast to the WHO's recommended levels

Leaching of rocks and minerals from the top layer of soil, and the oxidation processes (Dinka et al., 2015; Nikanorov., 2012). Table 5.1 shows the sulphate levels in the region's glacier streams which are graphically presented and compared with WHO standards in Fig 5.13. Sulfate concentration in 15% of the water samples is found below the detectable limit however remaining 34 samples have concentration less than 250

milligrams per liter, the maximum set by the WHO. The sulfate values for all the tested samples were ranged from 0-95.57 mg/l having a mean value of 22.10 mg/l.

5.6.5 Phosphate (PO_4^{2-})

Phosphorus naturally exists in mineral deposits and in rocks like apatite. Apatite is a group of phosphate minerals that includes calcium, iron, chlorine, and a number of other elements in various concentrations. As the mineralized phosphate complexes degrade naturally during weathering, the rocks progressively release the phosphorus as phosphate ions, which are soluble in water. Phosphates are not harmful to humans or animals unless they are present in extremely high concentrations (Archive Water Research Center - Phosphate in Water, 2022). Monitored values of phosphate for the collected water samples are introduced in the table 5.1 and graphically compared with World health Organization permissible limits in Fig 5.14. Surface water samples taken from the stations ST-13, ST-32, and ST-39 were exceeding the acceptable threshold value for PO_4 , which is 10 mg/l while the remaining 92.5% of the samples are within in the acceptable limits suggested by WHO. Overall, the phosphate concentrations range from 0-11.49 mg/l with an average value of 4.74 mg/l.

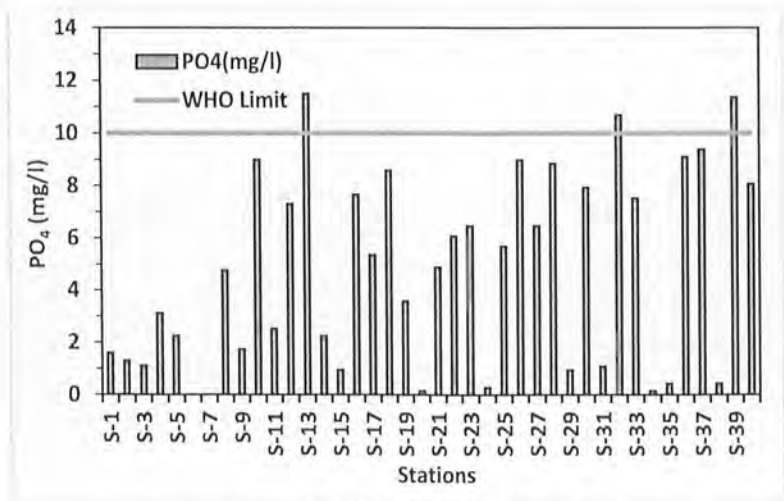
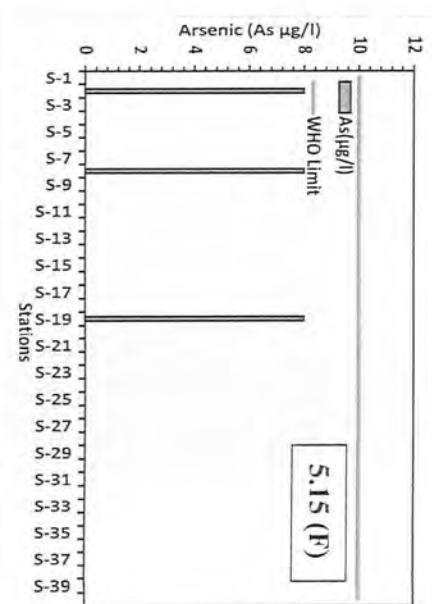
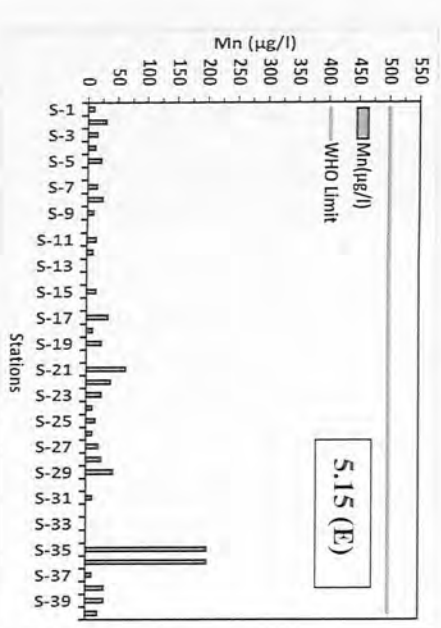
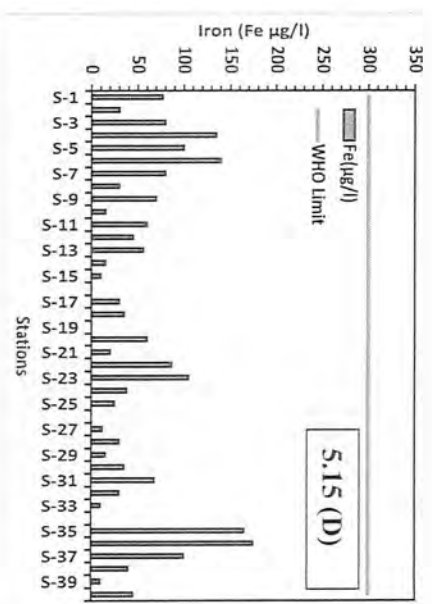
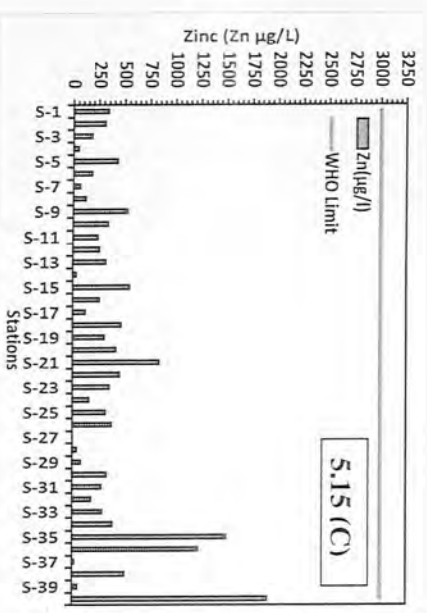
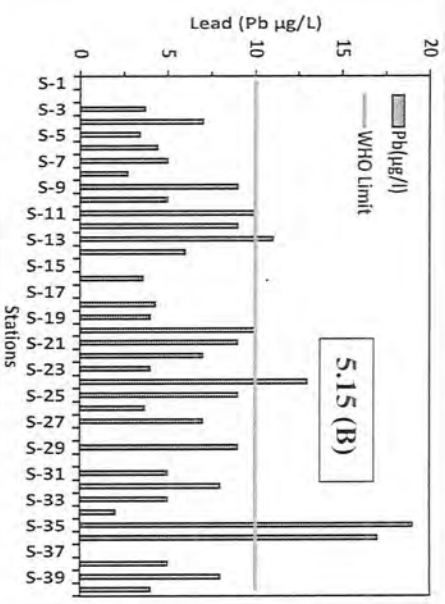
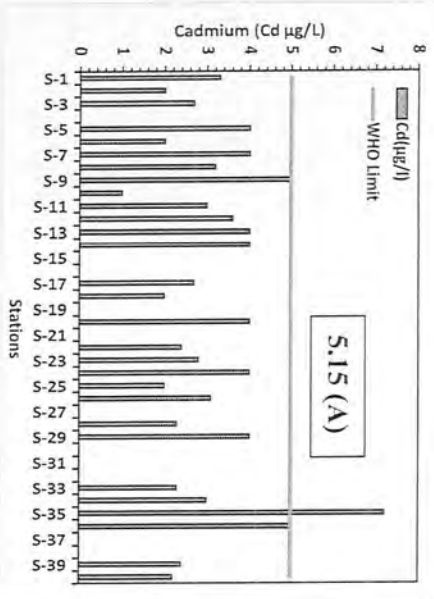


Fig 5. 14 Graph of Phosphate (PO_4^{2-}) for the Monitored Values of Physiochemical Parameters in Contrast to the WHO's recommended levels

Graphs for the monitored values Physiochemical parameters in contrast to the WHO's recommended level



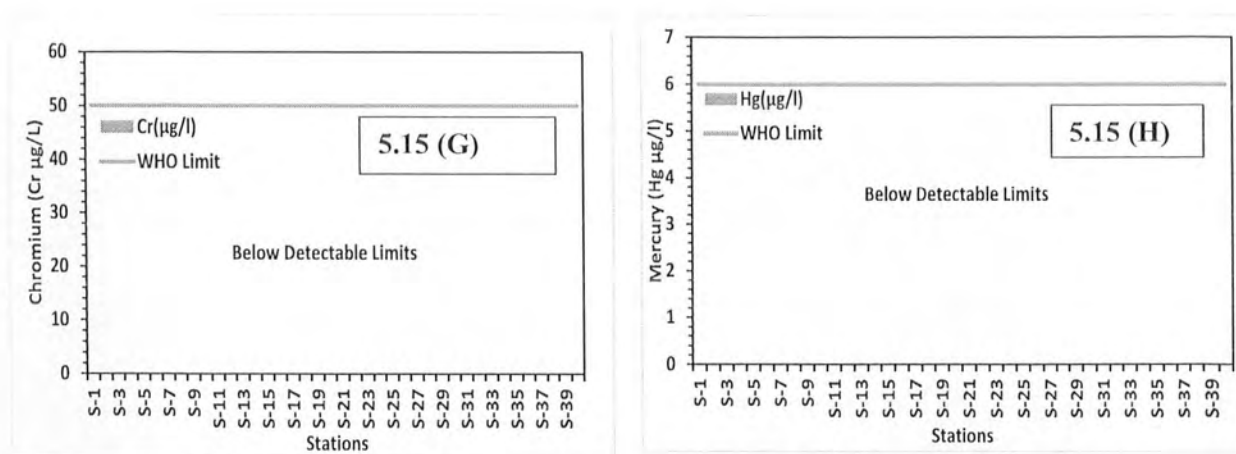


Fig 5. 15 Graphs for the Monitored Values of Physiochemical Parameters in Contrast to the WHO's recommended levels, (A) Cd, (B) Pb, (C) Zn, (D) Fe, (E) Mn, (F) As, (G) Cr and (H) Hg.

Table 5.2 Hydrogeochemical parameters of individual water sample and their concentration in the study area

S.No	pH	Turbidity	EC	TDS	TH	Na ⁺	K ⁺	Mg ²⁺	Ca ²⁺	Cl ⁻	HCO ₃	NO ₃ ⁻	PO ₄	SO ₄	WQI
ST - 1	8	105	180	102	264.7	21.18	16.95	17	78	63	220	1.30	1.60	0.00	71.31
ST - 2	7.4	2.25	230	161	393.9	35.00	26.92	21	72	45	310	0.37	1.30	0.00	25.75
ST - 3	8.29	8.08	80	53	383.3	12.00	9.70	9	44	55	110	0.75	1.11	0.80	23.23
ST - 4	8.14	5.15	110	81	332.6	18.00	11.04	7	85	75	165	0.70	3.11	0.85	22.92
ST - 5	8.5	1.49	170	96	385.3	16.37	10.63	10	49	58	134	0.00	2.26	0.70	23.29
ST - 6	8.2	2.36	78	44	188.7	10.24	5.70	8	45	46	97	0.44	0.00	0.00	17.96
ST - 7	8.03	2.05	135	96	406.8	11.21	8.83	13	71	64	173	0.00	0.00	0.22	23
ST - 8	8.11	3.17	75	53	203.5	13.26	9.70	10	53	43	140	0.90	4.77	0.00	24.5
ST - 9	7.5	4.27	210	137	464.2	19.16	6.07	15	87	39	266	0.00	1.74	0.22	30
ST - 10	7.79	3.88	100	67	249.4	13.46	6.98	9	72	58	138	0.00	9.00	0.00	21.37
ST - 11	7.9	3.17	163	96	373.6	15.24	9.70	11	84	77	167	0.53	2.53	0.00	26.13
ST - 12	7.3	1.63	102	69	463.8	16.21	8.60	27	102	98	232	0.22	7.31	3.59	29.25
ST - 13	7.4	1.53	113	73	480.6	12.43	9.51	14	83	63	177	0.77	11.49	1.76	30.17
ST - 14	6.8	1.8	132	85	299	15.26	8.79	15	95	95	210	2.30	2.26	58.55	24.5
ST - 15	8.54	8.1	90	52	199.4	17.24	9.70	9	65	70	150	1.11	0.94	0.22	16.37
ST - 16	7.23	83	108	62	273.8	13.29	10.60	18	80	55	170	2.90	7.66	52.38	58.74
ST - 17	7.06	4.32	64	47	290.8	11.43	9.77	8	71	52	147	0.57	5.37	3.69	18.54
ST - 18	8.05	39	94	68	236.7	13.29	10.60	12	75	95	130	0.00	8.59	0.51	40.23
ST - 19	8.7	2.56	66	42	328.3	15.24	13.32	11	86	82	170	0.00	3.58	3.40	22.74
ST - 20	7.24	90	133	85	344.7	15.26	12.42	13	94	67	147	0.67	0.15	64.24	69.19
ST - 21	7.86	19.26	60	33	282.6	15.26	23.30	10	85	85	87	1.33	4.90	72.53	31.63
ST - 22	7.75	2.63	100	62	406.8	18.18	37.34	19	100	66	179	0.00	6.08	89.32	28.65
ST - 23	7.3	1.5	125	81	398	15.26	38.71	25	103	80	190	2.33	6.48	95.57	28.13
ST - 24	6.9	56	84	57	207.6	7.37	14.23	11	65	55	150	3.00	0.29	84.97	53.07
ST - 25	8.14	26	115	82	232.6	5.39	13.32	11	75	95	170	2.76	5.69	24.61	36.22
ST - 26	7.5	126	147	89	303.3	7.37	19.67	13	100	80	200	3.40	8.98	3.21	83.78
ST - 27	7.9	16	78	46	203.1	14.26	16.86	14	52	63	115	0.00	6.48	4.27	25.32
ST - 28	8.6	5.41	264	170	191.2	33.00	11.51	7	59	58	145	0.00	8.85	12.85	22.21
ST - 29	8.48	19.28	145	102	215.8	37.87	14.76	11	54	73	134	0.80	0.94	16.71	33.64
ST - 30	8.18	9.36	200	134	257.6	31.50	10.51	11	61	43	140	0.00	7.93	41.20	22.11
ST - 31	8.11	17.02	194	107	199.4	15.26	11.51	9	65	85	130	0.00	1.08	2.53	24.85
ST - 32	7.98	2.41	192	112	270.1	7.37	15.14	11	90	70	110	1.30	10.70	54.60	24.6
ST - 33	7.91	1.84	187	100	211.9	13.29	9.70	9	70	60	141	0.69	7.53	4.27	21.15
ST - 34	6.75	2.07	196	121	228.3	9.34	7.88	13	70	55	130	0.56	0.15	45.92	18.1
ST - 35	8.77	1.26	607	385	423.2	125	21.27	10	56	97	298	0.00	0.42	12.46	53
ST - 36	8.83	1.67	633	389	365.8	111	22.75	11	80	106	297	0.00	9.11	15.78	51
ST - 37	8.27	4.46	70	52	207.6	36.97	9.70	11	57	55	110	0.00	9.38	49.58	19.87
ST - 38	7.73	1.52	415	277	236.5	21.18	11.51	15	70	85	140	0.87	0.42	45.63	21
ST - 39	8.14	7.44	85	58	270.1	31.05	9.70	11	55	63	133	2.76	11.35	0.03	28.15
ST - 40	7.8	1.1	102	67	276.9	11.32	15.86	19	55	69	127	1.48	8.06	16.71	24

Table 5. 3 Heavy metal concentration in ($\mu\text{g/L}$) for individual water sample of the study area

S.No	Cr	Pb	Cd	Cu	Zn	Fe	Hg	Mn	As	HPI
ST - 1	BDL	BDL	3.3	930	340	77	BDL	10	BDL	22.93
ST - 2	-	-	2	430	310	30	-	30	8	19.61
ST - 3	-	3.7	2.7	760	180	80	-	15	BDL	21.43
ST - 4	-	7	0	590	50.0	135	-	12	-	21.31
ST - 5	-	3.4	4	370	430	100	-	22	-	20.95
ST - 6	-	4.4	2	0	180	140	-	0	-	25.52
ST - 7	-	5	4	265	65	80	-	15	-	20.42
ST - 8	-	2.7	3.2	0	120	30	-	25	8	18.02
ST - 9	-	9	5	330	530	70	-	10	BDL	17.95
ST - 10	-	5	1	740	340	15	-	0	-	21.93
ST - 11	-	10	3	30	240	60	-	15	-	18.56
ST - 12	-	9	3.6	230	260	45	-	10	-	18.75
ST - 13	-	11	4	40	320	56	-	0	-	18.79
ST - 14	-	6	4	0	30	15	-	0	-	20.38
ST - 15	-	0	0	0	550	10	-	15	-	24.96
ST - 16	-	3.6	0	440	260	0	-	0	-	23.28
ST - 17	-	-	2.7	235	120	30	-	35	-	23.24
ST - 18	-	4.3	2	450	470	35	-	10	-	21.72
ST - 19	-	4	0	0	310	0	-	25	8	18.96
ST - 20	-	10	4	0	420	60	-	0	BDL	18.3
ST - 21	-	9	0	130	840	20	-	65	-	19.6
ST - 22	-	7	2.4	0	460	87	-	40	-	19.87
ST - 23	-	4	2.8	50	360	105	-	25	-	21.37
ST - 24	-	13	4	230	160	38	-	10	-	19.56
ST - 25	-	9	2	170	320	25	-	15	-	19.5
ST - 26	-	3.7	3.1	320	380	0	-	10	-	21.54
ST - 27	-	7	0	0	0	12	-	20	-	21.53
ST - 28	-	0	2.3	0	40	30	-	25	-	23.73
ST - 29	-	9	4	34	80	15	-	45	-	18.14
ST - 30	-	0	0	570	330	35	-	0	-	24.95
ST - 31	-	5	0	0	280	68	-	10	-	22.57
ST - 32	-	8	0	760	180	30	-	0	-	20.95
ST - 33	-	5	2.3	0	290	10	-	0	-	21.67
ST - 34	-	2	3	0	390	0	-	0	-	22.79
ST - 35	-	19	7.2	1380	1530	165	-	70	-	20.86
ST - 36	-	17	5	1180	1230	175	-	85	-	20.82
ST - 37	-	0	0	310	20	100	-	10	-	24.88
ST - 38	-	5	0	30	510	40	-	30	-	22.22
ST - 39	-	8	2.4	370	50	10	-	30	-	19.51
ST - 40	-	4	2.2	30	1900	45	-	20	-	21.86

5.7 EVALUATION OF WATER QUALITY

5.7.1 Water Quality Index (WQI)

The Water Quality Index is a useful tool for determining potable water quality and displaying the results in an understandable manner. In order to protect human health, it integrates all the parameters and compares them to the standards recommended by the government authorities. These indices provide a simple, unitless value that expresses water quality to the public or the authorities with ease. (Horton, 1965) created the first WQI model in the literature by statistically categorizing the water quality index. Brown (1965) made additional modifications in conjunction with the National Sanitation Foundation water quality index (NSFWQ).

WQI is a robust mathematical approach for simplifying and presenting massive amounts of water quality information as a single value and to create an in-depth assessment of the groundwater quality (Ramakrishnaiah et al., 2009; Varol & Davraz, 2015). Scientists throughout the world utilize WQIs to evaluate the Safety of drinking water across various geological settings (Adimalla et al., 2018; Aly et al., 2015; Ramakrishnaiah et al., 2009). For the current study, each monitored water quality parameter is assessed to determine the suitability of the collected water samples for drinking purpose. The key physiochemical variables used for the computation of WQI included EC, pH, turbidity, hardness, TDS, Ca^{+2} , Mg^{+2} , K^{+} , Na^{+2} , SO_4^{2-} , NO_3^{-} , Cl^{-} , HCO_3^{-} , PO_4^{-} , Cr, Pb, Cd, Zn, Fe, Hg, Mn, and As respectively. The water quality index was computed using the four steps listed below:

1. In the first step each physiochemical characteristic was assigned a weight according to its proportionate influence on the overall quality of water suitable for human consumption. The following formula is used to determine the relative weight (W_i):

$$W_i = \frac{w_i}{\sum_{i=1}^n w_i} \quad (2)$$

whereas, " W_i " is the relative weight, " w_i " represents the weight of each parameter and " n " is the number of total parameters

2. The observed value of each physical and chemical parameter is divided by its corresponding (WHO, 2022) standard, and the resulting percentage is used to create a quality rating scale (Q_i), where 100 represents the optimal level of quality.

$$Q_i = \frac{C_i}{S_i} \times 100 \quad (3)$$

Whereas, " C_i " represents the measured value of the parameters in mg/l and " S_i " are the WHO standard

3. Depending on the value of each indicator of water quality, " SI " was calculated in the WQI's final step by multiplying the relative weight (W_i) with the quality rating scale (Q_i). The water quality index is equal to the sum of " SI ".

$$SI = W_i Q_i \quad (4)$$

$$WQI = \sum SI_i \quad (5)$$

The most significant step in determining a physiochemical parameter's significance for drinking purposes is to assign weights to each chemical parameter. Each of the 23 parameters has been given a weight (w_i) based on its relative significance to the overall quality of potable water, as indicated in the table (5.4). The weights of the parameters range from 2 for the least significant to 5 for the most significant.

Table 5. 4 Relative Weight of Physic-Chemical Parameters

Chemical Parameter	WHO Standard (2022)	Weight (wi)	Relative Weight (Wi)
PH	8.5	4	0.05
Turbidity (NTU)	5	2	0.02
EC (µs/cm)	1000	4	0.05
TDS (mg/l)	1000	5	0.05
Cl ⁻ (mg/l)	250	4	0.05
Mg ⁺² (mg/l)	30	2	0.02
Ca ⁺² (mg/l)	300	2	0.02
Total Hardness	500	2	0.02
HCO ₃ ⁻ (mg/l)	500	3	0.04
Na ⁺² (mg/l)	100	3	0.04
K ⁺ (mg/l)	100	2	0.02
SO ₄ ²⁻ (mg/l)	250	5	0.06
PO ₄ ⁻ (mg/l)	10	3	0.04
NO ₃ ⁻ (mg/l)	50	5	0.06
Cr (mg/l)	0.05	5	0.06
Pb (mg/l)	0.01	5	0.06
Cd (mg/l)	0.005	5	0.06
Cu (mg/l)	2	2	0.02
Zn (mg/l)	3	3	0.04
Fe (mg/l)	0.3	4	0.05
Hg (mg/l)	0.006	5	0.06
Mn (mg/l)	0.5	4	0.05
As (mg/l)	0.01	5	0.06
		Σ wi = 84	Σ Wi =1

It is crucial to differentiate between the quality of groundwater and surface water utilized for drinking and for various other uses. WQI categorizes quality of water into qualitative words (such as excellent, good, medium, bad, and extremely poor) for the management and general public to take into consideration (A. K. Tiwari et al., 2018). For the current study, WQI value for all the collected water samples is determined and classification of the quality of the water is done using WQI suggested by (Adimalla et al., 2018; Kumar et al., 2019; R. N. Tiwari, 2011). Adimalla, 2019 recommendations were used to establish the standards for categorizing quality status of drinking water for the study region based on the WQI number. (Table 5.5)

Table 5. 5 Categorization of water quality status based on WQI value (after Adimalla et al., 2019)

WQI Value	Water Quality	Number of samples	% Samples
<25	Excellent	20	50
25-50	Good	13	32.5
50-100	Medium	7	17.5
100-150	Poor	0	-
>150	Extremely Poor	0	-

The measured WQI values for each of the 40 water samples fell into the excellent, good, and medium categories. Table 5.5 details the classification criteria for water samples that have been evaluated. Fig 5.16 and 5.17 shows that twenty of forty samples had values below 25, indicating that this was the case (i.e., excellent quality). Thirteen of the other twenty samples had WQI scores between 25 and 50 (considered to be of good quality), while the remaining seven had WQI values between 50 and 100. (i.e., medium quality). For most of the water samples' indicator values for the under examination physiochemical parameters were determined to be within acceptable limits since they derived from high-altitude, glacially-fed water channels and tributaries that are unlikely to contain dissolved or undissolved contaminants.

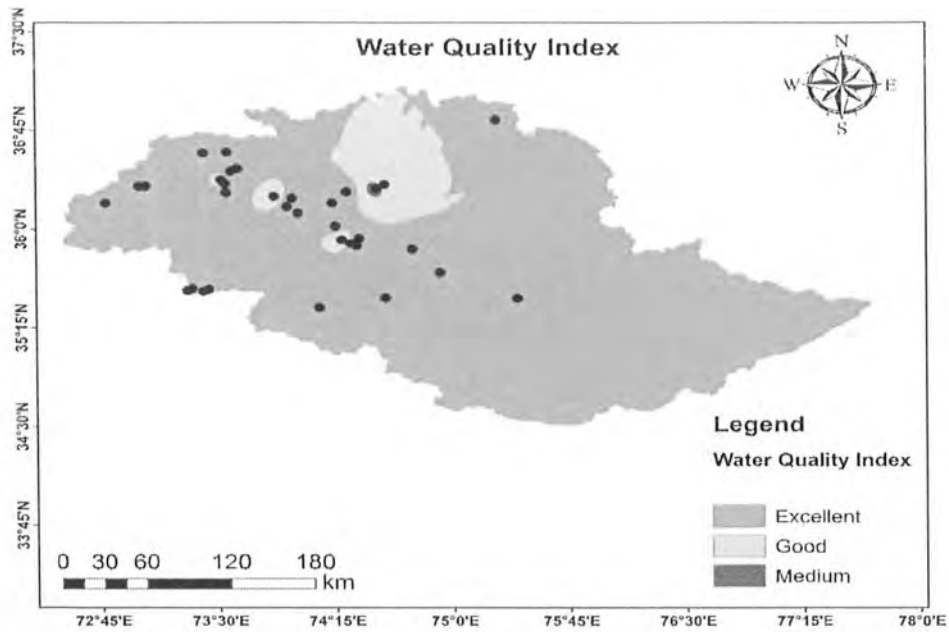


Fig 5. 16 The Water Quality Index Value of the Water Samples using GIS Map.

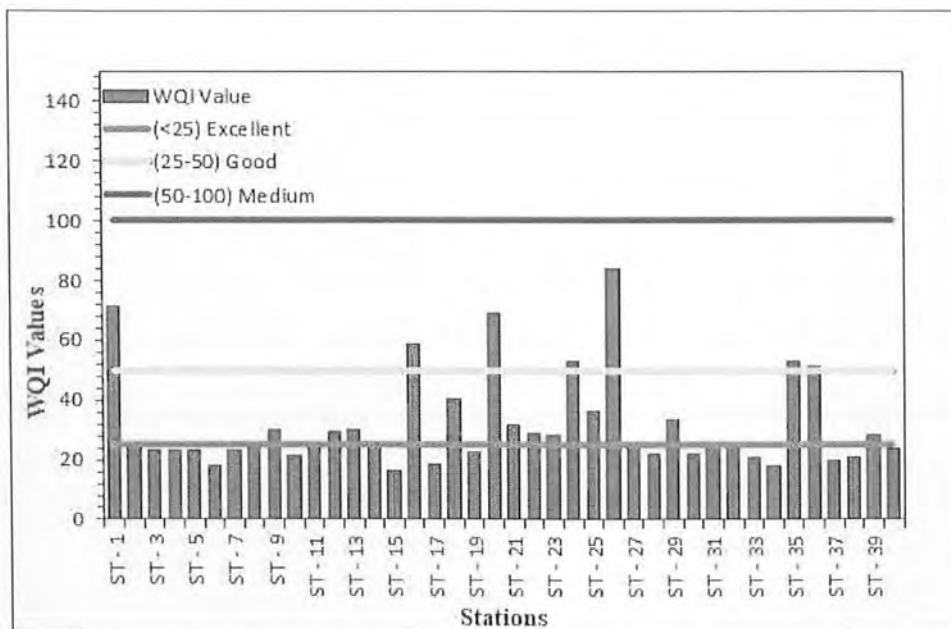


Fig 5. 17 Graph of The Water Quality Index Value of the Water Samples

5.7.2 Heavy Metal Pollution Index (HPI)

One of the world's problems is the poisoning of drinking water with HMs from both natural and man-made sources. In northern Pakistan, like in other rural areas, freshwater is essential for survival. It supports a variety of agro-pastoral livelihoods in addition to being used for consuming and other domestic needs (Baig et al., 2019). Surface waters in isolated regions of northern Pakistan with exposed geology and mineralized zones have rarely been reported to contain contaminated water and fish (Muhammad & Ahmad, 2020). In this context, it is crucial to monitor the level of heavy metal contamination in glacially supplied surface waters. The polluting variables that are observed for the evaluation of any system's quality provides information on the pollution exclusively in relation to that specific parameter. In order to acquire a composite effect of all pollution-related characteristics, quality indices are helpful (Prasad & Bose, 2001a). Recently, (Kumar et al., 2019; Prasad & Bose, 2001a) examined the heavy metal pollution index (HPI) and the amount of heavy metal contamination in both surface and groundwater. In the current investigation, the weighted arithmetic average mean technique of indexing was utilized to determine the total pollution produced by heavy metals in the samples which is developed by (Prasad & Bose, 2001b; Sheykhi & Moore, 2012). Nine heavy metal concentrations namely chromium (Cr), lead (Pb), zinc (Zn), cadmium (Cd), copper (Cu), iron (Fe), manganese (Mn), arsenic (As), and mercury (Hg) have been evaluated in water samples taken from glacier fed streams in the region.

The HPI measures the overall impact of individual HMs on the quality of surface water (Kumar et al., 2019; Sheykhi & Moore, 2012). Two basic steps are used to produce the HPI approach. The first step is to assign a weighting (Wi) to each

parameter. In addition, the index's foundational pollution parameter must be chosen. The rating scale is arbitrary, going from 0 to 1, and it's meant to indicate the relative weight of several quality characteristics. Setting values that are inversely proportional to the suggested standard for the relevant parameter might be used to evaluate it (Kumar et al., 2019; Prasad & Bose, 2001a; Sheykhi & Moore, 2012). The unit weightage (W_i) used in the calculation is considered to be inversely proportional to each heavy metal's the recommended standard value. Concentration limitations for this research (i.e., highest permitted value for drinking water (S_i) and the maximum desirable value (I_i) for each heavy metal were taken from (WHO, 2017). The HPI model suggested by (Mohan & Nithila, 1996) is given by:

$$HPI = \frac{\sum_{i=1}^n W_i \times Q_i}{\sum_{i=1}^n W_i} \quad (6)$$

Where, " Q_i " represents the Sub index of the i th parameter. and " W_i " represents unit weight of the i th parameter and " n " represents the number of parameters evaluated.

The sub index (Q_i) of the parameter is computed by,

$$Q_i = \sum_{i=1}^n \frac{|M_i - I_i|}{S_i - I_i} \times 100 \quad (7)$$

Where " M_i " is the measured value of i th parameter, " I_i " is the ideal value or highest desirable value of the i th parameter,

For any particular purpose, pollution indices are often calculated. The permitted or critical pollution index score for potable water is 100 in the suggested index; it is meant to measure the fitness of water quality of water for human use.

Table 5.6 Parameters for HMs in surface waters based on (WHO, 2017) recommendations for potable water

Sr #	Heavy Metals	Highest permitted value (<i>Si</i>)	Maximum desirable value (<i>Ii</i>)	Unit weight (<i>Wi</i>) =1/ <i>Si</i>
1	Cr (µg/l)	50	10	0.02
2	Pb (µg/l)	50	10	0.02
3	Cd (µg/l)	50	10	0.02
4	Cu (µg/l)	2000	1000	0.0005
5	Zn (µg/l)	3000	1000	0.0003
6	Fe (µg/l)	1000	100	0.001
7	Hg (µg/l)	60	10	0.016
8	Mn (µg/l)	300	100	0.003
9	As (µg/l)	50	10	0.02
10		-	-	∑ <i>Wi</i> = 0.1008

The monitored values of nine heavy metals (Cd, Cr, Cu, Cu, Zn, Fe, Hg, Mn, and As) have been considered while calculating the HPI of the water samples taken from the glacier-fed streams in the Gilgit river basin. In table 5.4, parameters for the computation of the HPI with unit weightages *Wi* and recommended limits are given for the region. Concerns may arise about the water's fitness for drinking if heavy metal concentrations in water systems exceed those that are normally anticipated (Gowd et al., 2008; Krishna & Govil, 2004; Romic et al., 2003).

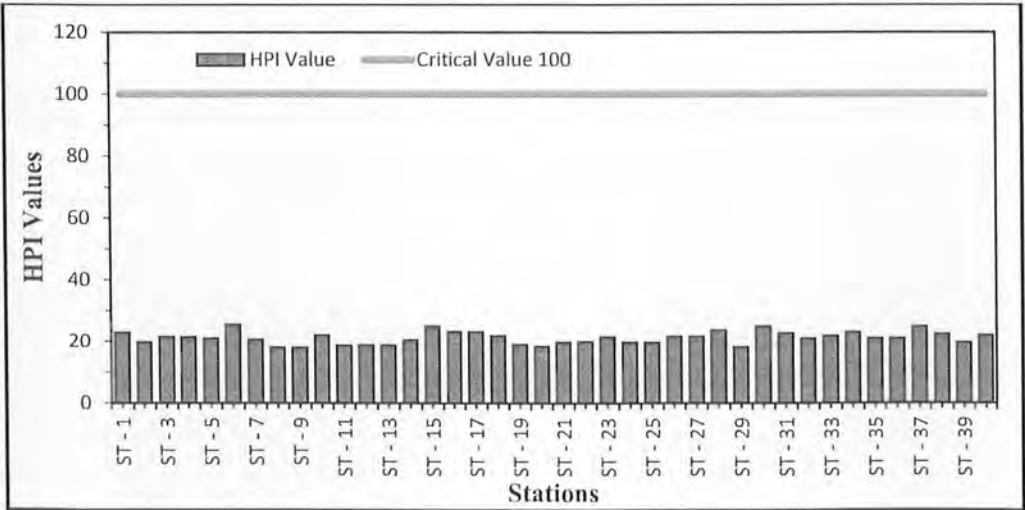


Fig 5. 18 Heavy Metal Pollution (HPI) Values for the Collected Water Samples

The computed HPI values for each of the forty samples ranged from a minimum of 17.95 to a high of 25.52, respectively as shown in Fig 5.18. The HPI value of all the water samples is far below the critical index value of 100, which indicating no contamination with heavy metals. It means the glacier fed water channels receives less pollutants from both geogenic and anthropogenic sources. This indicates a better water quality and safe for human consumption in the region.

5.8 WATER QUALITY ASSESSMENT FOR IRRIGATION PURPOSES

The quality of irrigation water indicates its mineral makeup and also shows how it affects the soil and plants. Depending on its origin, the varying geology of the region, and the weather patterns there, the composition of an area's irrigation water may vary widely (Khanoranga & Khalid, 2019). Agriculture is the predominant activity in the rock-dominated, arid areas of Gilgit Baltistan, where the main crops are wheat, maize, potato, and fruits such as cherry, apricot, and apples, which play a significant part in the region's economy. People of the area relies on the glacier melted waters for their irrigation purposes. Therefore, it is essential to analyze and evaluate the feasibility of water quality in the area for irrigation.

Irrigation water quality was evaluated through suitable parameters like sodium absorption ratio SAR (Varol & Davraz, 2015), residual sodium carbonate RSC (Raghunath, 1987; Eaton, 1950), sodium percentage %Na (Wilcox, 1955), permeability index PI (Doneen, 1964), and magnesium hazard ratio MHR (Adimalla, 2019; Raghunath, 1987) are calculated. For the current study, all ionic concentrations used in the computation are given in milliequivalents per liter (meq/L).

5.8.1 Sodium Absorption Ratio (SAR)

In respect to calcium and magnesium concentrations, the sodium absorption ratio (SAR) is a crucial indicator of the danger posed by sodium salt (Adimalla et al.,

2018; P. Li et al., 2018). For the reason that an excessive amount of salt may damage the soil's capacity to drain and its overall structure, Todd & Mays, 2004 came to the conclusion that the SAR evaluates how well water can be used for farming. SAR is computed using equation 8, proposed by (Patterson, 1994).

$$SAR = \frac{Na^{2+}}{\sqrt{\frac{Ca^{2+} + Mg^{2+}}{2}}} \quad (8)$$

The calculated values of SAR for collected water samples in the region ranges range from 0.11 – 3.03 with an average value and standard deviation of 0.48 and 0.55, respectively (table 5.7).

Richards (1954) had classified the surface water, based on SAR value and classification criteria are shown in the table 5.8. All of the obtained water samples were good quality for use in irrigation, as determined by the criteria, when the SAR value rises over 10, sodium salinity becomes a risk, slowing plant development by altering the nutritional ratio of calcium to magnesium which in-turn cause permeability problems in the soil (Adimalla, 2019; Khanoranga & Khalid, 2019).

5.8.2 Residual Sodium Carbonate

Around the globe, the residual sodium carbonate ratio is another measure of water quality used to determine whether or not water is suitable for irrigation (Selvakumar et al., 2017). High concentrations of weak acids (measured as the sum of carbonate and bicarbonate) in groundwater relative to alkaline earths (sum of calcium and magnesium) have a significant influence on the quality of water used for irrigation which is calculated by equation 9 (Raghunath, 1987; Eaton, 1950) and meq/L is used to express all concentrations..

$$RSC = [(HCO_3^- + CO_3^{2-}) - (Ca^{2+} + Mg^{2+})] \quad (9)$$

When carbonate and bicarbonate concentrations are greater than calcium and magnesium concentrations, the RSC value increases which causes the soil to become more alkaline and the adsorption of sodium in the soil increases. Due to increase in alkalinity the soil fertility decreases (Eaton, 1950). Table 5.7 provides a breakdown of the different types of irrigation water based on their respective RSC values. For the current study, RSC values range from -4.08 to 1.26 (table 5.8) with an average value of -1.98. Roughly 97.5 percent of the samples had RSC-classified values below 1.25 meq/L, indicating that they are of high enough quality for irrigation use while only 2.5% (1 water sample) has having values in between 1.25 and 2.5 represents doubtful nature for irrigation. High magnesium and calcium contents in the surface and groundwater are indicated by a negative RSC value. Thus, calcium and magnesium concentrations are essential in determining the quality of ground and surface water. Compared to calcium, magnesium can have more negative impacts on soil. Therefore, determining the magnesium hazard ratio is crucial.

5.8.3 Magnesium Hazard (MH)

Normally, the concentrations of Ca^{2+} and Mg^{2+} are usually well-balanced. The equilibrium can be disturbed occasionally by a high Mg^{2+} concentration, and an excess of Mg^{2+} can affect plant growth by making the water more alkaline. The MH value is calculated for the collected water samples in meq/L by using the equation 10 (Raghunath, 1987; Abdulhussein, 2018).

$$MH = \frac{Mg^{2+}}{(Ca^{2+} + Mg^{2+})} \times 100 \quad (10)$$

The high magnesium concentration in water raises its alkalinity, which negatively impacts agricultural yield. If the magnesium is in 50% excess, then the concentration of calcium in water than it retards the infiltration of soil and therefore it cannot attract clay particles. This action results in significant water adsorption between

the magnesium and clay fragments, which lowers the infiltration capacity of soil (Adimalla et al., 2018; Khanoranga & Khalid, 2019). The findings of the present investigation showed that the magnesium hazard (MH) values in table 5.7 the water samples ranged from 11.95 to 36.29 with an average value of 22.26 meq/L. All the samples of water from the region under investigation that were gathered met all requirements established for classification of water, table 5.8 in sense of the magnesium risk and hazard, making it completely suitable for agricultural use.

5.8.4 Sodium Percentage (Na%)

How much percentage of sodium salt is present in water is a major consideration when deciding whether it may be used for irrigation since it indicates the risk that sodium poses to the quality of irrigation water. High sodium concentrations in soil causes reduction in soil permeability which reduces the growth of plants (Alam et al., 2012; Wilcox, 1955). The equation 11 is utilized to calculate the sodium percentage of the water samples (Ghalib, 2017).

$$Na\% = \frac{Na^+ + K^+}{Ca^{2+} + Mg^{2+} + Na^+ + K^+} \times 100 \quad (11)$$

Sodium percentage in the water samples range from 11.01 to 62.32 with an average value of 22.26 (table 5.7). The water in the research region was categorized using the Na^+ (%) standard classification (table 5.8) several researchers have adopted (Islam et al., 2000; Srinivas et al., 2017).

5.8.5 Permeability Index (PI)

Another crucial factor to consider when determining if groundwater and surface water is suitable for irrigation purposes is the permeability index (PI). Use of mineral-rich (Na^+ , Ca^{2+} , Mg^{2+} , HCO_3^-) water for an extended period of time reduces soil permeability, which indirectly affects crop output (Singh et al., 2008). The equation 12

is used to calculate the permeability index in accordance with the (Doneen, 1964) standard requirements.

$$PI = \frac{(Na^+ + \sqrt{HCO_3^-})}{(Ca^{2+} + Mg^{2+} + Na^+)} \times 100 \quad (12)$$

Using irrigation over an extended period Soil aeration is hampered by mineral-rich water, which makes soil difficult to plough, and also affects seedling emergence. Overall, Plant growth is negatively impacted by decline in permeability index. PI scores of the area under study ranges between 21.50 to 39.34 with an average score of 30.51 table 5.7. Three classes were included in the Doneen classification for water based on PI levels i.e., good, suitable and unsuitable (table 5.8). According to PI classification for current study, 90% (36 samples) of the water samples had a value >75 depicts good class while the remaining four samples have values <25 shows unsuitable for irrigation based on PI values.

Table 5.7 Calculated Irrigation Water Quality Indices for the Region

Parameter(meq/L)	Range	Mean	Standard deviation
SAR	0.11-3.03	0.48	0.55
RSC	-4.08-1.26	-1.98	1.03
%Na	11.01-62.32	20.76	10.74
PI	21.50-39.34	30.51	4.21
MH	11.95-36.29	22.26	5.09

Table 5.8 Suitability of Surface Water for Irrigation Based on Various Classifications

Parameter	Range	Classification	No. of samples	% Samples
	0-10	Excellent	40	100
SAR	10-18	Good	-	-
	18-26	Doubtful	-	-
	>26	Unsuitable	-	-
	<20	Excellent	25	62.5
	20-40	Good	13	32.5
Na%	40-60	Permissible	1	2.5
	60-80	Doubtful	1	2.5
	>80	Unsuitable	-	-
	<1.25	Good	39	97.5
RSC	1.25-2.5	Doubtful	1	2.5
	>2.5	Unsuitable	-	-
MH	<50	Suitable	40	100
	>50	Unsuitable	-	-
	>75	Good	36	90
PI	25-75	Suitable	-	-
	<25	Unsuitable	4	10

5.9 THOSE REPORTED IN LITERATURE

Figures 5.19, 5.20 and 5.21 shows a comparison between the physiochemical parameters of the current study and those that have been published in the literature. Understanding the differences in water chemistry at various research locations is made possible by this comparison approach.

The comparison of the monitored physical parameter (i.e., pH, TDS, EC and turbidity) values of the water specimens are presented in Fig 5.19. The average pH was determined to be somewhat basic and higher than observed and published values in the

literature. This could come from the dissolution of carbonated rocks (Ahmed et al., 2021; Ali et al., 2016; Din, 2010; Hussain et al., 2015; Karim et al., 2014). For the current investigation, the average value of turbidity was found above the acceptable limit of the World Health Organization, which was in line with the majority of the results reported in previous studies (S. Ali et al., 2017; Shedayi et al., 2015; Sohail et al., 2019). In the downstream water presence of sediments, inorganic or organic content, and anthropogenic activity in the area, are all contributing factors to high levels of turbidity (Ahmed et al., 2021; Sohail et al., 2019). Compared to reported mean values in the literature, the mean conductivity value of the current study is said to be slightly lower.

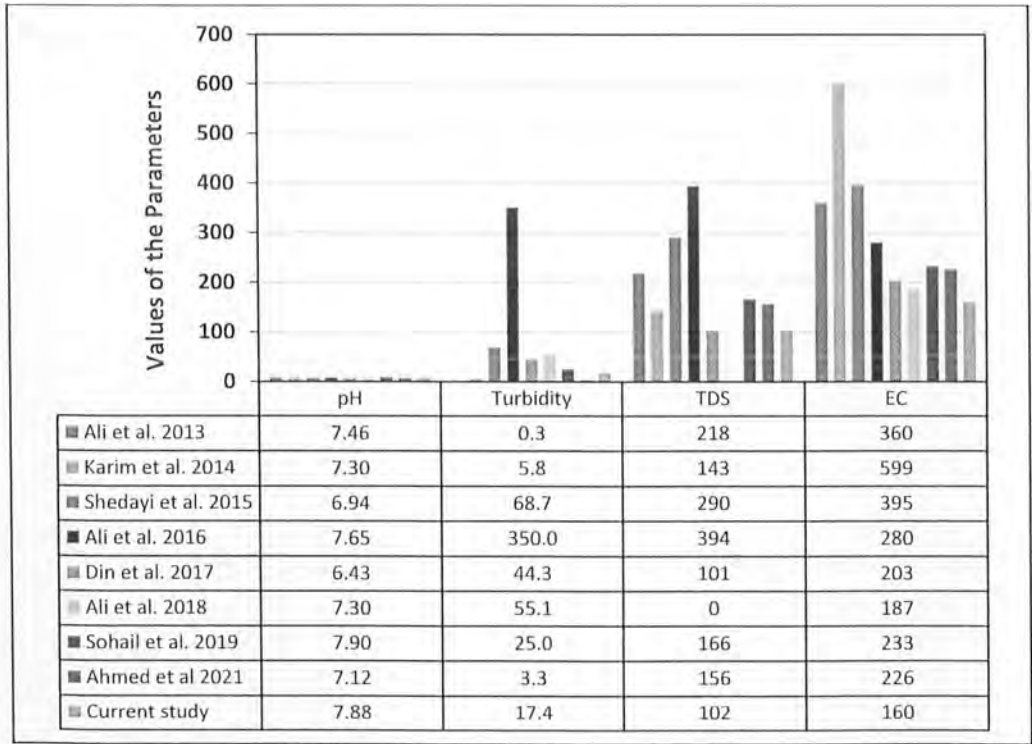


Fig 5. 19 Physical Properties of the Water Samples Compared to those in Published Research.

In comparison to the TDS values reported by A. Ali et al. (2016), Shedayi et al. (2015), Sohail et al. (2019), and Ahmed et al. (2021) for the water samples of Gilgit

river and glacier-fed streams they collected, the mean TDS value of the current study shown lower values.

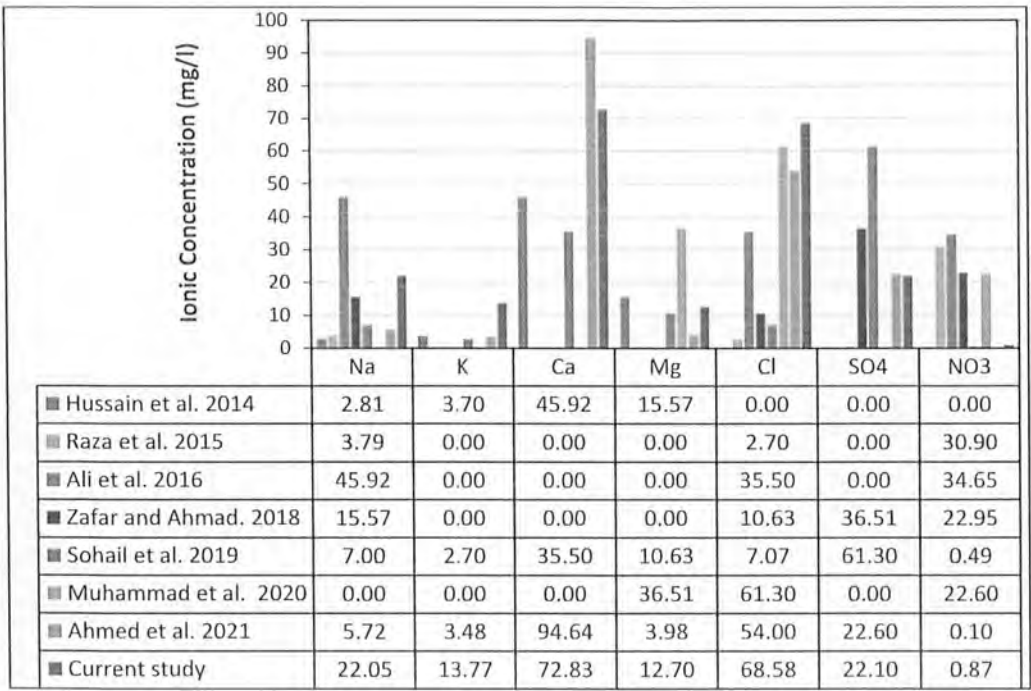


Fig 5. 20 Chemical Characteristics of the Water Samples Compared to Those in Published Research

Fig 5.20 displays the differences in the concentrations of anions and cations that were monitored in earlier research. The mean levels of the ions Na^+ , K^+ , and Cl^- were discovered to be higher than those noted in the data released by (Ahmed et al., 2021; Zafar and Ahmad 2018). The rapid disintegration of carbonate and silicate rocks may be the reason of the rise in these ions concentrations (Ahmed et al., 2021; Muhammad & Ahmad, 2020). The observed average values of Ca^{2+} ion was found lower as reported by Ahmed et al., (2021) and higher than the values published by (A. Ali et al., 2016; Sohail et al., 2019). The mean NO_3^- ion concentration in the area for the samples that were collected was much lower than the mean concentrations reported by (A. Ali et al., 2016; Zafar and Ahmad, 2018) and likely equivalent to the concentration previously

reported by Ahmed et al. (2021). This low level of NO_3^- is a result of decreased fertilizer usage in the upstream area, as excessive fertilizer use raises nitrate levels in water.

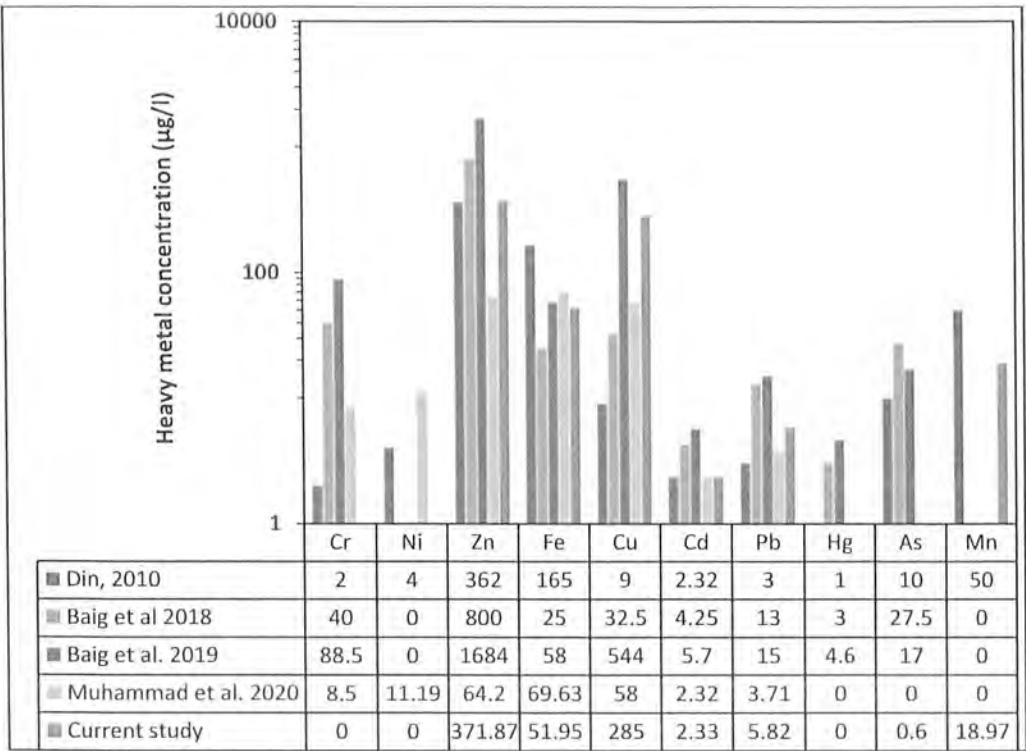


Fig 5. 21 Heavy metals of the water samples compared to those in published research.

Heavy metals including iron, zinc, manganese, and copper are essential for life at low concentrations despite their persistence, toxicity, and bio-accumulative nature but they have hazardous effects at large concentrations. The current study found that drinking water samples had mean concentrations of harmful heavy metals (i.e., Ni, Fe, Cu, and As) that were significantly lower than those previously reported by (Baig, Begum, Raut, et al., 2019; Islam-ud-Din, 2010; Muhammad & Ahmad, 2020). Islam-ud-Din, (2010) reported that there was a trace amount of Cr and Hg in the water, and High concentrations of chromium reported by (Baig, Begum, Khan, et al., 2017; Baig, Begum, Raut, et al., 2019) which exceeds the WHO permissible limits. The present investigation, states that the levels of Cr and Hg were all below the detectable limits.

Lack of upstream mining and farming might account for the lack of concentration. The mean value of Arsenic is also found comparatively very low in a few waters sample as reported in the literature.

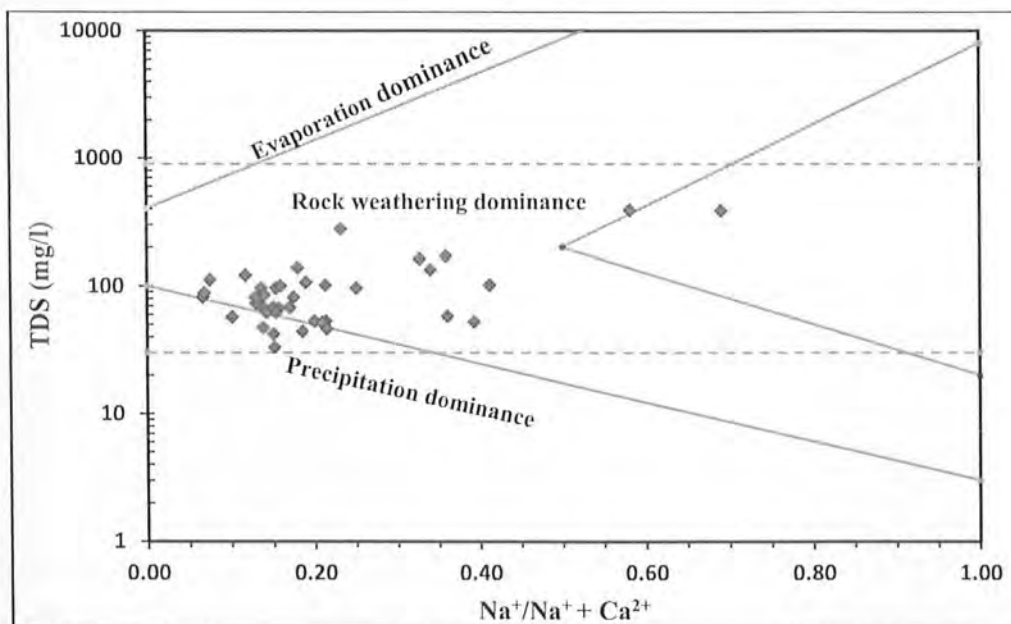
5.10 HYDRO-GEOCHEMICAL PROCESSES

5.10.1 Gibbs Plot

In order to analyze the geochemical processes involved in controlling the surface water chemistry (Gibbs, 1970) created a plot in the form of two semi-log diagrams, called Gibbs plot. Gibbs plot explains three main factors affecting water chemistry using analytical chemical data for multiple surface and underground water basins. Rock domination, evaporation crystallization, and atmospheric precipitation are the three major controlling factors. From bottom to top, the Gibbs plot (Fig 5.22) explains the governing factors: Precipitation dominance, rock dominance, and evaporation dominance. Specimens with a low TDS (0–10 mg/l), $\text{Na}^+ / (\text{Na}^+ + \text{Ca}^{2+})$, and $\text{Cl}^- / (\text{Cl}^- + \text{HCO}_3^-)$ ratios ranging from 0–1 typically fall on the bottom section of the plot, which reflects the precipitation dominance in governing the chemistry of water. The center-left portion of the plot, where water samples with medium concentrations of dissolved salts (70–300 mg/l), $\text{Na}^+ / (\text{Na}^+ + \text{Ca}^{2+})$, and $\text{Cl}^- / (\text{Cl}^- + \text{HCO}_3^-)$ ratio < 0.5 , indicates the dominance of rock weathering. When the ratio of the $\text{Na}^+ / (\text{Na}^+ + \text{Ca}^{2+})$, and $\text{Cl}^- / (\text{Cl}^- + \text{HCO}_3^-)$ between (0.5–1) and the dissolved salt value increases over 300.0 mg/l, the dominance of evaporation takes place (Rehman Qaisar et al., 2018; Stallard & Edmond, 1987).

All of the water samples from the research region that were analyzed in this study were found to be inside the rock weathering dominant zone. This indicates that the rock dissolution can highly influence the water chemistry of glacier fed streams. In terms of the region's geology, the area under investigation is dominated by silicate rocks

i.e., granite, carbonate rocks, basalts, and schists (Ahmed et al., 2021). The rock-water interaction results in the disintegration of the minerals found in the rocks which is the main source of TDS, Mg^{2+} , Ca^{2+} , Na^+ , Cl^- , HCO_3^{2-} and other dissolved ions in the glacial-fed surface water of the region under study. To determine the primary influencing variables on surface and groundwater chemistry, the Gibbs diagram is frequently utilized in many regions around the globe (Adimalla et al., 2018; P. Li et al., 2016; Rehman Qaisar et al., 2018; Towfiqul Islam et al., 2017). These demonstrate that the interaction between rock and water is one of the most significant and dominant variables controlling the surface water chemistry in the studied region.



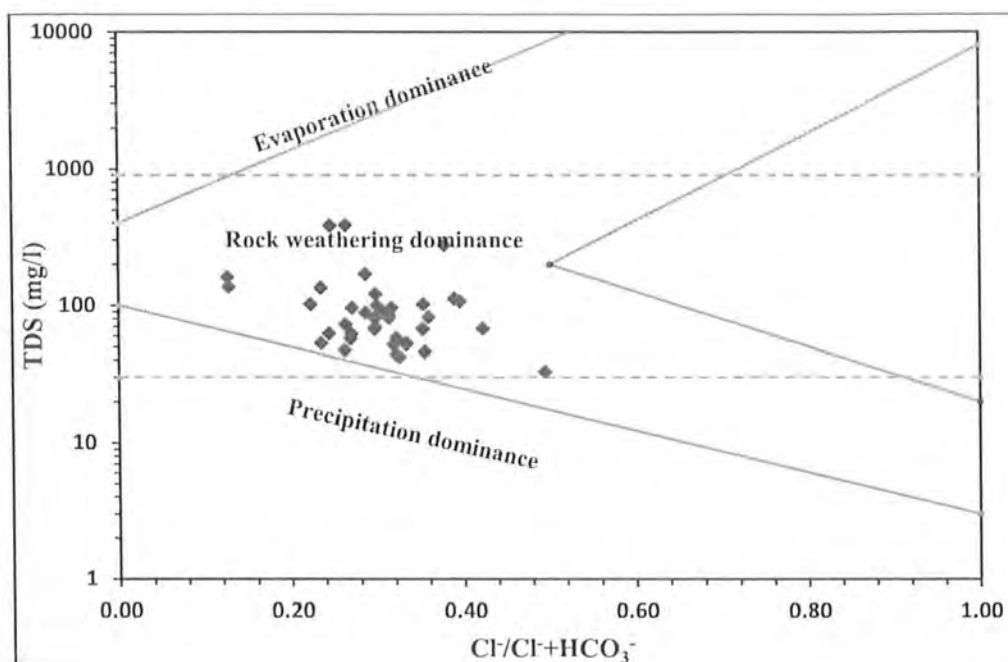


Fig 5. 22 Gibbs Plot Showing (a) TDS vs $\text{Na}^+/\text{Na}^+ + \text{Ca}^{2+}$, (b) TDS vs $\text{Cl}^-/\text{Cl}^- + \text{HCO}_3^-$
Showing Dominance of Rock Weathering

5.11 CHARACTERIZATION OF GEOCHEMICAL FACIES AND HYDROCHEMICAL WATER TYPES

5.11.1 Piper Graphical Plot

To get a deeper understanding of the sources of dissolved components in water, (Piper, 1944) suggested an efficient graphic procedure. Since most water in its natural state is thought to include cations and anions in a condition of chemical equilibrium, this method was developed. The three cations that are thought to be most abundant are calcium (Ca^{2+}), magnesium (Mg^{2+}), and sodium (Na^{2+}) while Bicarbonate (HCO_3^-), sulphate (SO_4^-), and chloride are the three most dominant anions (Cl^-). Together with the main three anions and cations, less frequent anion and cation components are added. Piper, (1944) recommended drawing two triangles that represent the cations and anions, respectively, and one central diamond that summarizes both triangles in order to form a graph containing the main components of water. The cations are represented by the

left triangle, and the anions are represented by the right one. The axis for calcium forms the base of the cation triangle, while the sides on the left and right represent magnesium and sodium, respectively. In the case of the anion, the base serves as the axis for the ion chloride, right side for carbonate + bicarbonate, while the left side serves as the axis for SO_4 ions. The hydro-Chemical facies can be identified based on location of the sample. Geo-chemical facies are the chemically-based diagnostic feature of water solutions that occur in hydrologic systems, and they are described in the Fig 5.23. Analytical values are taken in the units of (Milli- equivalent %).

The concentration of cations and ions in the research region is depicted in great detail by the piper trilinear diagram utilized for the current study, as seen in Fig 5.23. The bulk of the representative samples are located to the left corner of the cation triangle, where the Ca^{2+} values are ($> 50\%$), indicating the predominance of calcium over magnesium and Alkalis (Na^+ and K^+). Two samples are located in the central portion of the cation triangle, showing no cation dominance, and two samples are located in the right-hand corner, showing an elevated concentration of the ions Na^+ and K^+ . This demonstrates the impact of local Na^+ and K^+ sources (A. Karim et al., 2000.; Rehman Qaisar et al., 2018; Selemani et al., 2017). To the contrary, approximately half of the samples in the triangle of anions are on the left side of the triangle, indicating that HCO_3^- predominates over Cl^- and SO_4^{2-} . Of the samples, 27% are in the middle of the triangle, indicating that no single anion is predominate. Higher Cl^- and SO_4^{2-} concentrations in two samples on the right side of the triangle may have their origins in a combination of geological and anthropogenic sources (Rehman Qaisar et al., 2018; Xiao et al., 2012).

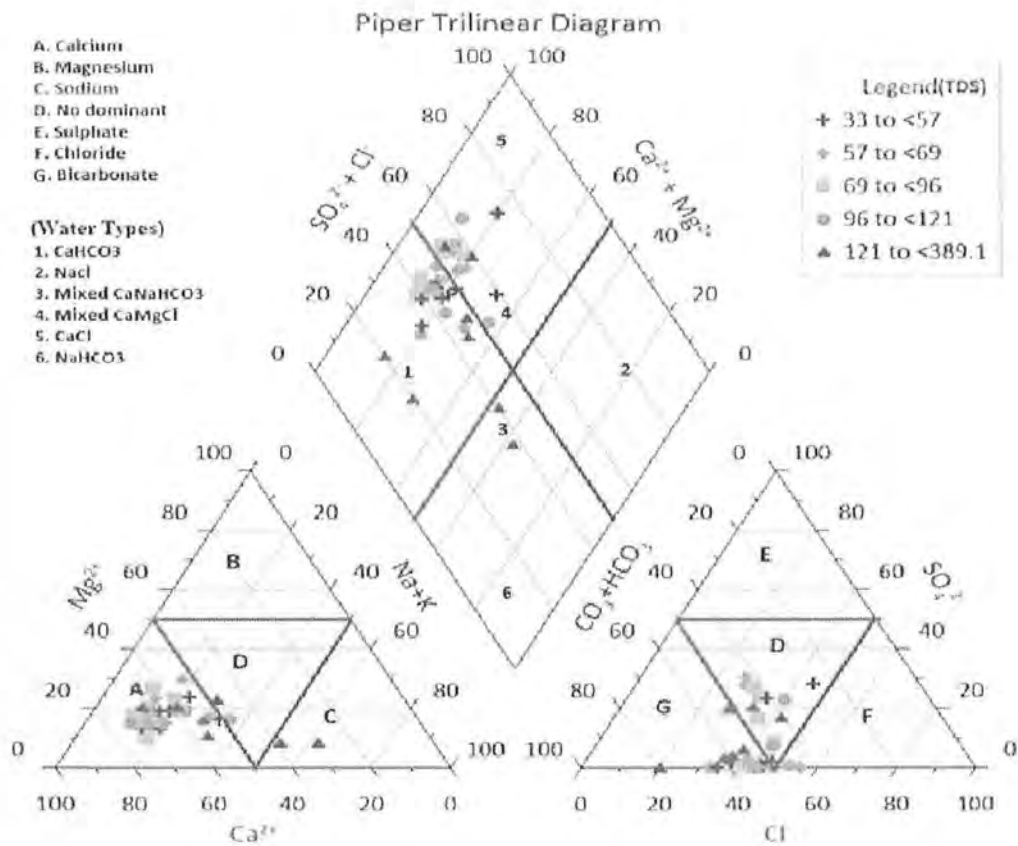


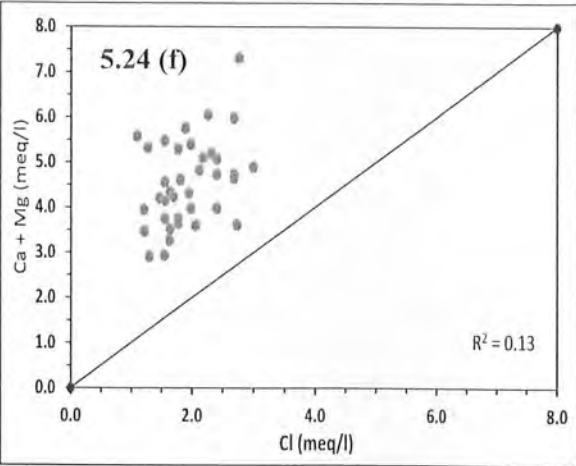
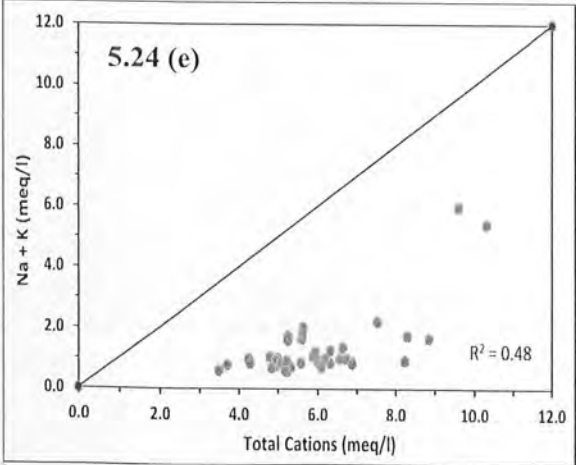
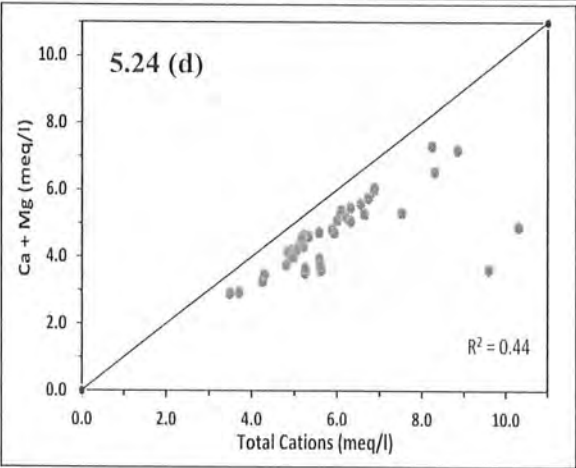
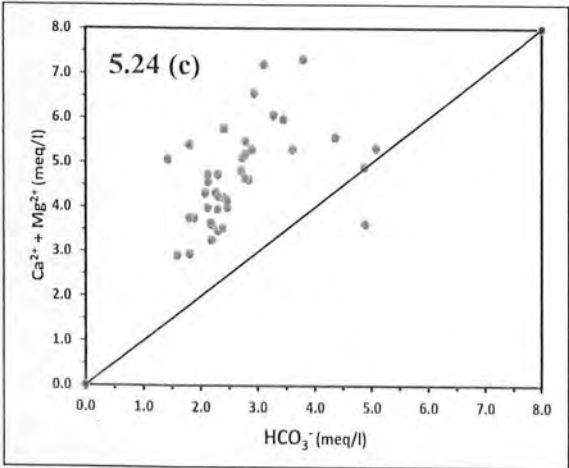
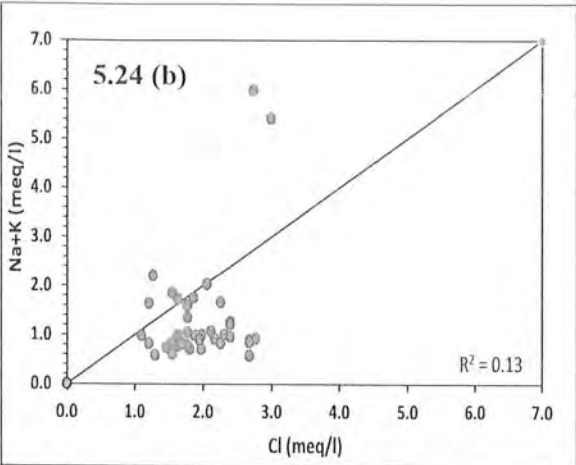
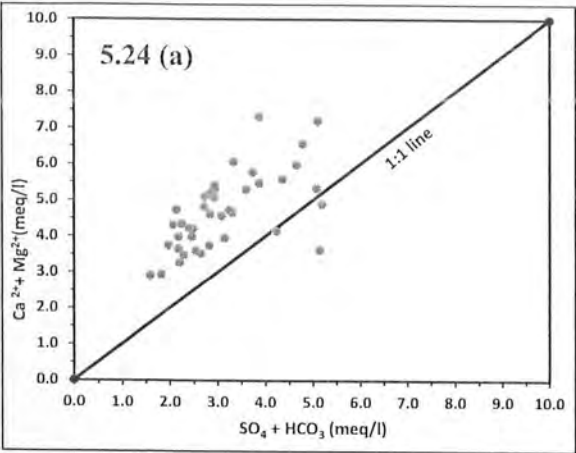
Fig 5. 23 Piper Diagram for Surface Water of the Study Region

The diamond ring of Piper diagram has six subfields (Fig 5.22): (1) Ca-HCO_3 , (2) NaCl , (3) Mixed Ca-Na-HCO_3 , (4) Mixed Ca-Mg-Cl (5) Ca-Cl , (6) Na-H-CO_3 (Adimalla, 2019; Ismail & Ahmed, 2021; Manoj et al., 2013). These subfields categorize the water by deducing its hydrogeochemical parameters and describing the predominant cations and anions that affect the local hydrochemistry (Walton, 1970; Rehman Qaisar et al., 2018). The samples plotted in the subfields 1, 4 and 5 for the study area shows that in 38 water samples alkaline earth elements exceeds alkalis while only 2 samples showing excess of alkalis over alkaline earth elements i.e., shown in subfield 2, 3 and 6. This indicates that alkaline earth metals, rather than alkali metals, are prevalent in the area's surface water, as predicted by the geochemical facies in the piper diagram. The samples plotted on piper plot of the study area also showed that

about 60% of the water samples are Ca-HCO₃ type and 25% are classified as Mixed Ca-Mg-Cl type. Carbonate weathering, in addition to a mixing mechanism and a cation exchange process, is hypothesized to regulate the chemistry of glacier-fed water (Murad et al., 2011; Oinam et al., 2012). Two samples have the water type Ca-Cl, whereas the other two display a mixed Ca-Na-HCO₃ water type.

5.12 IONIC RATIOS

The weathering of various rocks can produce a variety of significant ion combinations. For instance, the weathering of carbonates yields Mg²⁺, Ca²⁺, and HCO₃⁻; that of silicates yields Si, Na⁺, K⁺, Ca²⁺, Mg²⁺, and HCO₃⁻; while that of evaporites yields mostly SO₄²⁻, Ca²⁺, Mg²⁺, Na⁺, K⁺, Cl⁻, and NO₃⁻ (A. Karim et al., 2000; Rehman Qaisar et al., 2018). In addition, halite, pyrite, and sulphate minerals like gypsum and anhydrite dissolve and release Na⁺, Cl⁻, and SO₄²⁻ into the water. So, overall, the concentration of chemical constituents depends upon the weathering of rocks when the water interacts with them.



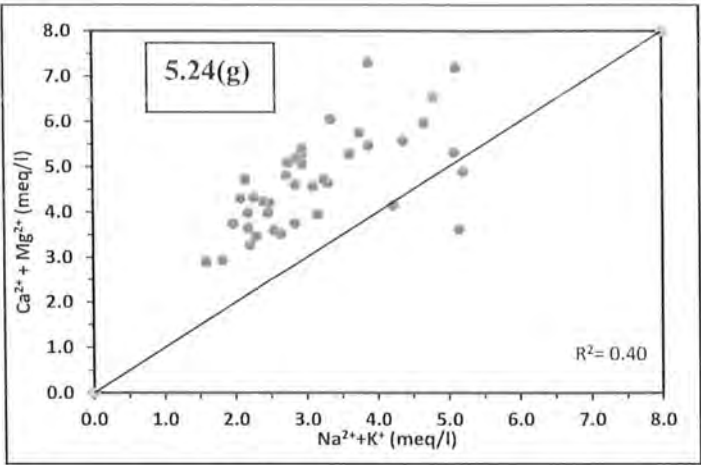


Fig 5. 24 Scatter Plots Showing the Variability in Ionic Concentrations of Water Samples

Ionic ratios have been extensively employed by a variety of researchers as a tool for elucidating hydrogeochemical processes involving both surface and underground water resources (Ahmed et al., 2021; Rehman Qaisar et al., 2018). For 92% of the samples Fig 5.24(a), the dissolving of calcite (CaCO_3), gypsum ($\text{CaSO}_4 \cdot 2\text{H}_2\text{O}$), and dolomite $\text{CaMg}(\text{CO}_3)_2$, for the study region is shown in the plot of $(\text{Ca}^{2+} + \text{Mg}^{2+})$ versus $(\text{HCO}_3^- + \text{SO}_4^-)$ for surface water, samples were dispersed (above 1:1 line) along the left side in the plot (Ahmed et al., 2021; Liu et al., 2015; Rehman Qaisar et al., 2018; Zhang et al., 2021) . Three samples having a ratio below 1:1 trend line is indicative of silicate rock weathering. (Asare-Donkor et al., 2018). It means, the dominant hydrogeochemical process in the study region is thus carbonate dissolution. The ratio of $(\text{Na}^+ + \text{K}^+)/\text{Cl}^-$ is greater than 1, which indicates that the weathering and disintegration of silicate minerals is a more significant contributor to the enrichment of Na^+ and K^+ ions in the water. (Lin et al., 2016). Range of the ratio of $(\text{Na}^+ + \text{K}^+)/\text{Cl}^-$ for the collected water specimens is in the range of 0.21 to 2.18, with a mean value of 0.68. The ratios for six water samples are predicted to be higher than 1 (plotted above 1:1 line). The remaining 85% of the samples have a ratio of less than 1 (below the 1:1 line in Fig 5.24b), which shows that the sources of Cl^- in the water samples were ion

exchange and the dissolution of minerals that contained chloride. In the present study, carbonate rock weathering has a relatively greater impact on the overall water chemistry than weathering of silicate rocks. The $\text{Ca}^{2+} + \text{Mg}^{2+}/\text{HCO}_3^-$ ratio may be used to identify the origin sources of Ca^{2+} , Mg^{2+} , and HCO_3^- (see fig 5.24c). High ratios of $(\text{Ca}^{2+} + \text{Mg}^{2+})/(\text{HCO}_3^-)$ was found for the water samples, where 97.5% values exceed the trend line of 1:1. This suggests that carbonate weathering is the controlling factor of Ca^{2+} , Mg^{2+} and HCO_3^- . The ratio of $(\text{Ca}^{2+} + \text{Mg}^{2+}) / (\text{total cation})$ in (Fig 5.24d) ranges from 0.37 to 0.88 with a mean value of 0.79 and majority of the samples are plotted just under the 1:1 line. These low ratios also validate the dissolution of carbonate rocks. The ratio of $\text{Na}^{2+} + \text{K}^+$ vs total cation in (Fig 5.24e) ranges from 0.11 to 0.62 (plotted far below the 1:1 line) suggests less contribution of silicate weathering and high carbonate weathering (Rehman Qaisar et al., 2018). The ratio of $(\text{Ca}^{2+} + \text{Mg}^{2+})/\text{Cl}^-$ in all the collected samples was found greater than (Fig 5.24f) indicates that the high concentration of Ca^{2+} and Mg^{2+} was caused by the weathering of carbonate rocks.

The $(\text{Ca}^{2+} + \text{Mg}^{2+})/(\text{Na}^+ + \text{K}^+)$ ratio (Fig 5.24g) is frequently used to assess the relative contributions of various rock types in a sedimentary basin (Ahmad et al., 1998; Han & Liu, 2004; Rehman Qaisar et al., 2018; S.-R. Zhang et al., 2007). The ratio of $(\text{Ca}^{2+} + \text{Mg}^{2+})/(\text{Na}^+ + \text{K}^+)$ is high in water bodies where carbonates are the main source, reaching 6.0 in a portion of the Indus River of India (Ahmad et al., 1998). In this study, the study region lies in carbonate weathering zone where 92% of the water samples lies (above 1:1 line).

6 CONCLUSION

The surface water of Gilgit Baltistan, which is fed by glaciers, is an important natural resource for human consumption and agricultural use. The water quality of glacial fed streams is evaluated for drinking and agricultural use based on their physicochemical parameters. This study involves a data set of 23 water quality parameters for 40 collected water samples. The measured physio-chemical quality parameters were measured as follows: turbidity 1.1–126, conductivity 60–633 ($\mu\text{S}/\text{cm}$), (NTU), hardness 188–480 (mg/L), pH 6.7–8.8, TDS 33–389 (mg/L), Ca^{2+} 44–103 (mg/L), K^{+} 5.7–38.71 (mg/L), Mg^{2+} 7–27 (mg/L), Na^{+} 5.4–125 (mg/L), Cl^{-} 39–106 (mg/L), SO_4^{2-} 0–95.57 (mg/L), NO_3^{-} 0–3.40 (mg/L). In addition to parameters 9 heavy metal parameters were also determine to analyze the heavy metals pollution in the surface water. The measured values of these heavy metals recorded as follows: Pb 0–19 ($\mu\text{g}/\text{L}$), Cd 0–7.2 ($\mu\text{g}/\text{L}$), Cu 0–1380 ($\mu\text{g}/\text{L}$), Zn 0–1900 ($\mu\text{g}/\text{L}$), Fe 0–175 ($\mu\text{g}/\text{L}$), Mn 0–85 ($\mu\text{g}/\text{L}$), As 0–8 ($\mu\text{g}/\text{L}$), while Cr and Hg were below the detectable limits. All the measured values are then compared with the given WHO standards and the concentration levels of majority of parameters were found within the allowable limits except a few parameters in a few samples are exceeding the given limits. All of the water samples that were examined had an estimated ion charge balance error (ICBE) of $\pm 10\%$ that was recoded with an average value of 6.58.

Using the WQI approach, all 40 collected samples were examined to determine their status of quality status. Overall, twenty samples were classified as excellent (50%), thirteen samples as good (32.5%), and seven as moderate (17.5%) quality for drinking use. Heavy metal pollution index is employed to assess the heavy metal pollution levels. Results presented that, HPI values of all the 100% samples are far below the critical value of 100 indicating safe for human consumption. Similar to this, the suitability of the surface water for irrigation was determined using indicators for the purpose of

irrigation quality such as RSC, SAR, PI, Na (%) and MH hazard. The outcomes of all the indicators revealed that surface water of the area suitable for irrigation purpose and falls in excellent to good quality. Gibbs plot is employed to determine the main controlling mechanism of the water chemistry. The results exhibit that all of the samples fell in rock dominance block, which indicates the dissolution of rocks mainly control the chemistry of glacier fed water. The results of Gibbs plot and ion ratios effectively depicts that weathering of carbonate rocks has a great impact as compared to weathering of silicate rocks in controlling the water chemistry. The piper plot showed that, hydrochemically 60% of the water samples are Ca-HCO_3 type while the remaining are Ca-Cl type, Mixed Ca-Mg-Cl type, and Ca-Na- HCO_3 water type.

7 RECOMMENDATIONS

- The water quality of study area is successfully evaluated by laboratory examinations, statistical and machine learning techniques. The physic-chemical concentrations in water resources are changed with changing seasons and climate. Therefore, it is recommended to conduct a time series study to analyze the variability in water quality parameters in the hilly areas.
- This research can be extended to other regions of the area.
- Pakistan's Gilgit-Baltistan province needs environmental protection regulations from the local administration. Uncontrolled human activities degrade downstream waters. Improved garbage disposal, anthropogenic activity monitoring, and local cleanliness are required. Clean and safe water should be provided in more inventive and sustainable ways.

BIBLIOGRAPHY

- Abro, M. I., Wei, M., Zhu, D., Elahi, E., Ali, G., Khaskheli, M. A., ... & Nkunjimana, A. (2020). Hydrological evaluation of satellite and reanalysis precipitation products in the glacier-fed river basin (Gilgit). *Arabian Journal of Geosciences*, 13, 1-13.
- Adimalla, N. (2020). Heavy metals contamination in urban surface soils of Medak province, India, and its risk assessment and spatial distribution. *Environmental Geochemistry and Health*, 42(1), 59-75.
- Adimalla, N., Li, P., & Venkatayogi, S. (2018). Hydrogeochemical evaluation of groundwater quality for drinking and irrigation purposes and integrated interpretation with water quality index studies. *Environmental Processes*, 5, 363-383.
- Adnan, M., Nabi, G., Kang, S., Zhang, G., Adnan, R. M., Anjum, M. N., ... & Ali, A. F. (2017). Snowmelt Runoff Modelling under Projected Climate Change Patterns in the Gilgit River Basin of Northern Pakistan. *Polish Journal of Environmental Studies*, 26(2).
- Islam-ud-Din, Shah, M. T., & Khan, S. (2010). Hydro-chemical investigations of high altitude alpine lakes of Gilgit and Ghizar districts, Gilgit-Baltistan, Pakistan. *JOURNAL OF HIMALAYAN EARTH SCIENCES*, 43, 35-35.
- Adnan, M., Nabi, G., Poomee, M. S., & Ashraf, A. (2017). Snowmelt runoff prediction under changing climate in the Himalayan cryosphere: A case of Gilgit River Basin. *Geoscience Frontiers*, 8(5), 941-949.
- Ahmad, T., Khanna, P. P., Chakrapani, G. J., & Balakrishnan, S. (1998). Geochemical characteristics of water and sediment of the Indus river, Trans-Himalaya, India:

- constraints on weathering and erosion. *Journal of Asian Earth Sciences*, 16(2-3), 333-346.
- Ahmed, M. F., Waqas, U., Khan, M. S., Rashid, H. M. A., & Saqib, S. (2021). Evaluation and classification of water quality of glacier-fed channels using supervised learning and water quality index. *Water and Environment Journal*, 35(4), 1174-1191.
- Alam, M., Rais, S., & Aslam, M. (2012). Hydrochemical investigation and quality assessment of ground water in rural areas of Delhi, India. *Environmental Earth Sciences*, 66, 97-110.
- Ali, A., Hussain, K., Hussain, J. S., & Hussain, N. (2016). Drinking water quality analysis of water supply network at Ganish Valley Hunza Nagar, Gilgit Baltistan, Pakistan. *International Research Journal of Environmental Sciences*, 5(3), 54-62.
- Ali, A., Hussain, K., Hussain, J. S., & Hussain, N. (2016). Drinking water quality analysis of water supply network at Ganish Valley Hunza Nagar, Gilgit Baltistan, Pakistan. *International Research Journal of Environmental Sciences*, 5(3), 54-62.
- Esmaeili, M., Salimi, A., Drebenstedt, C., Abbaszadeh, M., & Aghajani Bazzazi, A. (2015). Application of PCA, SVR, and ANFIS for modeling of rock fragmentation. *Arabian Journal of Geosciences*, 8, 6881-6893.
- Amin, A., Iqbal, J., Asghar, A., & Ribbe, L. (2018). Analysis of current and future water demands in the Upper Indus Basin under IPCC climate and socio-economic scenarios using a hydro-economic WEAP model. *Water*, 10(5), 537.
- Appiah-Opong, R., Ofori, A., Ofosuhenne, M., Ofori-Attah, E., Nunoo, F. K., Tuffour, I., ... & Fosu-Mensah, B. Y. (2021). Heavy metals concentration and pollution index (HPI) in drinking water along the southwest coast of Ghana. *Applied Water*

Science, 11, 1-10.

- Asare-Donkor, N. K., Ofori, J. O., & Adimado, A. A. (2018). Hydrochemical characteristics of surface water and ecological risk assessment of sediments from settlements within the Birim River basin in Ghana. *Environmental Systems Research*, 7(1), 1-17.
- Baig, S., Begum, F., Khan, M. Z., Mumtaz, S., Shedayi, A. A., Wafee, S., ... & Ali, H. (2019). A human health risk assessment of heavy metals in drinking water systems of Central-Hunza, Gilgit-Baltistan, Pakistan. *Fresenius environmental bulletin*, 28(3), 2269-2277.
- Bhutani, R., Pande, K., & Venkatesan, T. R. (2009). ^{40}Ar – ^{39}Ar dating of volcanic rocks of the Shyok suture zone in north–west trans-Himalaya: Implications for the post-collision evolution of the Shyok suture zone. *Journal of Asian Earth Sciences*, 34(2), 168-177.
- Debernardi, L., De Luca, D. A., & Lasagna, M. (2008). Correlation between nitrate concentration in groundwater and parameters affecting aquifer intrinsic vulnerability. *Environmental Geology*, 55, 539-558.
- Dinka, M. O., Loiskandl, W., & Ndambuki, J. M. (2015). Hydrochemical characterization of various surface water and groundwater resources available in Matahara areas, Fantalle Woreda of Oromiya region. *Journal of Hydrology: Regional Studies*, 3, 444-456.
- Domenico, P. A., & Schwartz, F. W. (1997). *Physical and chemical hydrogeology*. John Wiley & sons.
- Faisal, N., & Gaffar, A. (2012). Development of Pakistan's new area weighted rainfall using Thiessen polygon method. *Pakistan Journal of Meteorology (Pakistan)*.

- Fatima, S. U., Khan, M. A., Siddiqui, F., Mahmood, N., Salman, N., Alamgir, A., & Shaukat, S. S. (2022). Geospatial assessment of water quality using principal components analysis (PCA) and water quality index (WQI) in Basho Valley, Gilgit Baltistan (Northern Areas of Pakistan). *Environmental Monitoring and Assessment*, 194(3), 151.
- Fatima, S. U., Khan, M. A., Siddiqui, F., Mahmood, N., Salman, N., Alamgir, A., & Shaukat, S. S. (2022). Geospatial assessment of water quality using principal components analysis (PCA) and water quality index (WQI) in Basho Valley, Gilgit Baltistan (Northern Areas of Pakistan). *Environmental Monitoring and Assessment*, 194(3), 151.
- Gibbs, R. J. (1970). Mechanisms controlling world water chemistry. *Science*, 170(3962), 1088-1090.
- Srinivasa Gowd, S., & Govil, P. K. (2008). Distribution of heavy metals in surface water of Ranipet industrial area in Tamil Nadu, India. *Environmental monitoring and assessment*, 136, 197-207.
- Han, G., & Liu, C. Q. (2004). Water geochemistry controlled by carbonate dissolution: a study of the river waters draining karst-dominated terrain, Guizhou Province, China. *Chemical Geology*, 204(1-2), 1-21.
- Hussain, T., Sheikh, S., Kazami, J. H., Hussain, M., Hussain, A., Hassan, N. U., ... & Khan, H. (2014). Geo-spatial assessment of tap water and air quality in Gilgit city using geographical information system. *J Biodivers Environ Sci*, 5(6), 49-54.
- Islam, M. R., Lahermo, W. P., Salminen, R., Rojstaczer, S., & Peuraniemi, V. (2000). Lake and reservoir water quality affected by metals leaching from tropical soils, Bangladesh. *Environmental Geology*, 39, 1083-1089.

- Ismail, S., & Ahmed, M. F. (2021). GIS-based spatio-temporal and geostatistical analysis of groundwater parameters of Lahore region Pakistan and their source characterization. *Environmental Earth Sciences*, 80, 1-26.
- Iturrizaga, L. (2005). Historical glacier-dammed lakes and outburst floods in the Karambar valley (Hindukush-Karakoram). *GeoJournal*, 63, 1-47.
- Jeelani, G. H., Bhat, N. A., Shivanna, K., & Bhat, M. Y. (2011). Geochemical characterization of surface water and spring water in SE Kashmir Valley, western Himalaya: Implications to water-rock interaction. *Journal of earth system science*, 120, 921-932.
- Karim, A., & Veizer, J. (2000). Weathering processes in the Indus River Basin: implications from riverine carbon, sulfur, oxygen, and strontium isotopes. *Chemical Geology*, 170(1-4), 153-177.
- Karim, R., Nafees, M. A., Khan, T., Khan, M. Z., Wafi, S., & Ali, S. (2014). Studies in assessment of environmental degradation and tourism in the Karakoram Mountain Ranges using water quality characterization. *Journal of Biodiversity and Environmental Sciences*, 5(2), 260-267.
- Kavurmaci, M., & Üstün, A. K. (2016). Assessment of groundwater quality using DEA and AHP: a case study in the Sereflikochisar region in Turkey. *Environmental monitoring and assessment*, 188, 1-13.
- Khan, H., & Baig, S. (2017). High altitude wetlands of the HKH region of northern Pakistan—status of current knowledge, challenges and research opportunities. *Wetlands*, 37(2), 371-380.
- Khan, N., Shahid, S., Ismail, T., Ahmed, K., & Nawaz, N. (2019). Trends in heat wave related indices in Pakistan. *Stochastic environmental research and risk assessment*,

33, 287-302.

Khan, S., Javed, Z. H., Wahid, A., Ranjha, A. N., & Hasan, M. U. (2020). *Climate of the Gilgit-Baltistan Province , Pakistan. 11*(3).

Khalid, S. (2019). An assessment of groundwater quality for irrigation and drinking purposes around brick kilns in three districts of Balochistan province, Pakistan, through water quality index and multivariate statistical approaches. *Journal of Geochemical Exploration*, 197, 14-26.

Khelifi, R., & Hamza-Chaffai, A. (2010). Head and neck cancer due to heavy metal exposure via tobacco smoking and professional exposure: a review. *Toxicology and applied pharmacology*, 248(2), 71-88.

Krishna, A. K., & Govil, P. K. (2004). Heavy metal contamination of soil around Pali industrial area, Rajasthan, India. *Environmental Geology*, 47, 38-44.

Kumar, V., Parihar, R. D., Sharma, A., Bakshi, P., Sidhu, G. P. S., Bali, A. S., ... & Rodrigo-Comino, J. (2019). Global evaluation of heavy metal content in surface water bodies: A meta-analysis using heavy metal pollution indices and multivariate statistical analyses. *Chemosphere*, 236, 124364.

Laar, C., Akiti, T. T., Brimah, A. K., Fianko, J. R., Osae, S., & Osei, J. (2011). Hydrochemistry and isotopic composition of the Sakumo Ramsar site. *Research Journal of Environmental and Earth Sciences*, 3(2), 146-152.

Li, P., Wu, J., & Qian, H. (2016). Hydrochemical appraisal of groundwater quality for drinking and irrigation purposes and the major influencing factors: a case study in and around Hua County, China. *Arabian Journal of Geosciences*, 9, 1-17.

Li, P., Wu, J., Tian, R., He, S., He, X., Xue, C., & Zhang, K. (2018). *Geochemistry*,

- hydraulic connectivity and quality appraisal of multilayered groundwater in the Hongdunzi Coal Mine, Northwest China. *Mine Water and the Environment*, 37(2), 222-237.
- Li, S., Xu, Z., Wang, H., Wang, J., & Zhang, Q. (2009). Geochemistry of the upper Han River basin, China: 3: Anthropogenic inputs and chemical weathering to the dissolved load. *Chemical Geology*, 264(1-4), 89-95.
- Lin, M. L., Peng, W. H., & Gui, H. R. (2016). Hydrochemical characteristics and quality assessment of deep groundwater from the coal-bearing aquifer of the Linhuan coal-mining district, Northern Anhui Province, China. *Environmental monitoring and assessment*, 188, 1-13.
- Liu, F., Song, X., Yang, L., Han, D., Zhang, Y., Ma, Y., & Bu, H. (2015). The role of anthropogenic and natural factors in shaping the geochemical evolution of groundwater in the Subei Lake basin, Ordos energy base, Northwestern China. *Science of the Total Environment*, 538, 327-340.
- Murad, A. A., Garamoon, H., Hussein, S., & Al-Nuaimi, H. S. (2011). Hydrogeochemical characterization and isotope investigations of a carbonate aquifer of the northern part of the United Arab Emirates. *Journal of Asian Earth Sciences*, 40(1), 213-225.
- Nakhaei, M., Amiri, V., Rezaei, K., & Moosaei, F. (2015). An investigation of the potential environmental contamination from the leachate of the Rasht waste disposal site in Iran. *Bulletin of engineering geology and the environment*, 74, 233-246.
- Stumm, W., Morgan, J. J., & Drever, J. I. (1996). Aquatic chemistry. *Journal of environmental quality*, 25(5), 1162.

- Oinam, J. D., Ramanathan, A. L., & Singh, G. (2012). Geochemical and statistical evaluation of groundwater in Imphal and Thoubal district of Manipur, India. *Journal of Asian Earth Sciences*, 48, 136-149.
- Piper, A. M. (1944). A graphic procedure in the geochemical interpretation of water-analyses. *Eos, Transactions American Geophysical Union*, 25(6), 914-928.
- Parsad, B., & Bose, J. M. (2001). Evaluation of heavy metal pollution index for surface and spring water near a limestone mining area of the lower Himalayas. *Environmental Geology*, 41(183), 8.
- Prasad, B., & Bose, J. (2001). Evaluation of the heavy metal pollution index for surface and spring water near a limestone mining area of the lower Himalayas. *Environmental Geology*, 41(1-2), 183-188.
- Psenner, R., & Catalan, J. (1994). Chemical composition of lakes in crystalline basins: a combination of atmospheric deposition, geologic background, biological activity and human action..
- Ramakrishnaiah, C. R., Sadashivaiah, C., & Ranganna, G. (2009). Assessment of water quality index for the groundwater in Tumkur Taluk, Karnataka State, India. *E-Journal of chemistry*, 6(2), 523-530.
- Rehman, K., Fatima, F., Waheed, I., & Akash, M. S. H. (2018). Prevalence of exposure of heavy metals and their impact on health consequences. *Journal of cellular biochemistry*, 119(1), 157-184.
- Rehman Qaisar, F. U., Zhang, F., Pant, R. R., Wang, G., Khan, S., & Zeng, C. (2018). Spatial variation, source identification, and quality assessment of surface water geochemical composition in the Indus River Basin, Pakistan. *Environmental Science and Pollution Research*, 25, 12749-12763.

- Romic, M., & Romic, D. (2003). Heavy metals distribution in agricultural topsoils in urban area. *Environmental geology*, 43, 795-805.
- Selemani, J. R., Zhang, J., Muzuka, A. N., Njau, K. N., Zhang, G., Maggid, A., ... & Pradhan, S. (2017). Seasonal water chemistry variability in the Pangani River basin, Tanzania. *Environmental Science and Pollution Research*, 24, 26092-26110.
- Selemani, J. R., Zhang, J., Muzuka, A. N., Njau, K. N., Zhang, G., Maggid, A., ... & Pradhan, S. (2017). Seasonal water chemistry variability in the Pangani River basin, Tanzania. *Environmental Science and Pollution Research*, 24, 26092-26110.
- Shedayi, A. A., Nazia, J., & Saba, R. (2015). Drinking water quality status in Gilgit, Pakistan and WHO standards. *Science International (Lahore)*, 27(3, Section A), 2305-2311.
- Sheykhi, V., & Moore, F. (2012). Geochemical characterization of Kor River water quality, fars province, Southwest Iran. *Water quality, exposure and health*, 4, 25-38.
- Singh, A. K., Mondal, G. C., Kumar, S., Singh, T. B., Tewary, B. K., & Sinha, A. (2008). Major ion chemistry, weathering processes and water quality assessment in upper catchment of Damodar River basin, India. *Environmental geology*, 54(4), 745-758.
- Sinyukovich, V. N. (2003). Relationships between water flow and dissolved solids discharge in the major tributaries of Lake Baikal. *Water Resources*, 30, 186-190.
- Sohail, M. T., Aftab, R., Mahfooz, Y., Yasar, A., Yen, Y., Shaikh, S. A., & Irshad, S. (2019). Estimation of water quality, management and risk assessment in Khyber

- Pakhtunkhwa and Gilgit-Baltistan, Pakistan. *Desalination and Water Treatment*, 171, 105-114.
- Soomro, B. (2004). Paddy and water environment related issues, problems and prospects in Pakistan. *Paddy and Water Environment*, 2, 41-44.
- Srinivas, Y., Aghil, T. B., Hudson Oliver, D., Nithya Nair, C., & Chandrasekar, N. (2017). Hydrochemical characteristics and quality assessment of groundwater along the Manavalakurichi coast, Tamil Nadu, India. *Applied Water Science*, 7, 1429-1438.
- Davies, D., Jindal-Snape, D., Digby, R., Howe, A., Collier, C., & Hay, P. (2014). The roles and development needs of teachers to promote creativity: A systematic review of literature. *Teaching and Teacher Education*, 41, 34-41.
- Tiwari, A. K., & Singh, A. K. (2014). Hydrogeochemical investigation and groundwater quality assessment of Pratapgarh district, Uttar Pradesh. *J Geol Soc India*, 83(3), 329-343.
- Tiwari, A. K., Singh, A. K., & Mahato, M. K. (2018). Assessment of groundwater quality of Pratapgarh district in India for suitability of drinking purpose using water quality index (WQI) and GIS technique. *Sustainable water resources management*, 4, 601-616.
- Tiwari, R. N. (2011). Assessment of groundwater quality and pollution potential of Jawa block Rewa district, Madhya Pradesh, India. *Proceedings of the international academy of ecology and environmental sciences*, 1(3-4), 202.
- Towfiqul Islam, A. R. M., Shen, S., Bodrud-Doza, M. D., & Safiur Rahman, M. (2017). Assessing irrigation water quality in Faridpur district of Bangladesh using several indices and statistical approaches. *Arabian journal of geosciences*, 10, 1-25.

- Trauth, R., & Xanthopoulos, C. (1997). Non-point pollution of groundwater in urban areas. *Water research*, 31(11), 2711-2718.
- Varol, S., & Davraz, A. (2015). Evaluation of the groundwater quality with WQI (Water Quality Index) and multivariate analysis: a case study of the Tefenni plain (Burdur/Turkey). *Environmental earth sciences*, 73, 1725-1744.
- Machado, A., Amorim, E., & Bordalo, A. A. (2022). Spatial and Seasonal Drinking Water Quality Assessment in a Sub-Saharan Country (Guinea-Bissau). *Water*, 14(13), 1987.
- Xiao, J., Jin, Z. D., Ding, H., Wang, J., & Zhang, F. (2012). Geochemistry and solute sources of surface waters of the Tarim River Basin in the extreme arid region, NW Tibetan Plateau. *Journal of Asian Earth Sciences*, 54, 162-173.
- Zanotti, C., Rotiroti, M., Fumagalli, L., Stefania, G. A., Canonaco, F., Stefenelli, G., ... & Bonomi, T. (2019). Groundwater and surface water quality characterization through positive matrix factorization combined with GIS approach. *Water research*, 159, 122-134.
- Zhang, Q., Qian, H., Xu, P., Hou, K., & Yang, F. (2021). Groundwater quality assessment using a new integrated-weight water quality index (IWQI) and driver analysis in the Jiaokou Irrigation District, China. *Ecotoxicology and environmental safety*, 212, 111992.

APPENDIX

Calculation Of Water Quality Index

Station I	WHO Standard (Si)	Monitored value (Ci)	Weight (wi)	Relative weight (Wi)	$qi = Ci/Si \times 100$	$Wi \times qi$
PH	8.5	8	4	0.047619048	94.11764706	4.481792717
Turbidity (NTU)	5	105	2	0.023809524	2100	50
EC(μ s/cm)	1000	180	4	0.047619048	18	0.857142857
TDS(mg/l)	1000	102	5	0.05952381	10.2	0.607142857
CL-(mg/l)	250	63	4	0.047619048	25.2	1.2
Mg+2(mg/l)	30	17	2	0.023809524	56.66666667	1.349206349
Ca+2(mg/l)	300	78	2	0.023809524	26	0.619047619
Total Hardness	500	264.7	2	0.023809524	52.94	1.26047619
HCO3-(mg/l)	500	220	3	0.035714286	44	1.571428571
Na+2(mg/l)	100	21.18	3	0.035714286	21.18421053	0.756578947
K+2(mg/l)	100	16.95	2	0.023809524	16.95054945	0.403584511
SO4(mg/l)	250	0.00	5	0.05952381	0	0
PO4(mg/l)	10	1.60	3	0.035714286	16.03302881	0.572608172
NO3(mg/l)	50	1.30	5	0.05952381	2.6	0.154761905
Cr(mg/l)	0.05	0	5	0.05952381	0	0
Pb(mg/l)	0.01	0	5	0.05952381	0	0
Cd(mg/l)	0.005	0.0033	5	0.05952381	66	3.928571429
Cu(mg/l)	2	0.93	2	0.023809524	46.5	1.107142857
Zn(mg/l)	3	0.34	3	0.035714286	11.33333333	0.404761905
Fe(mg/l)	0.3	0.077	4	0.047619048	25.66666667	1.222222222
Hg(mg/l)	0.006	0	5	0.05952381	0	0
Mn(mg/l)	0.5	0.01	4	0.047619048	2	0.095238095
As(mg/l)	0.01	0	5	0.05952381	0	0
			84	1	WQi	70.5917022

Calculation of Heavy Metal Pollution Index

ST - I	Standard Permissible limit (Si)	Ideal Value (Ii)	Monitored Value (Mi)	$Wi = 1/Si$	$(Mi - Ii)$	$ (Mi - Ii) $	$Si - Ii$	$Qi = (Mi - Ii)/(Si - Ii) \times 100$	$Wi \times Qi$
Cr(μ g/l)	50	10	0	0.02	-10	10	40	25	0.5
Pb(μ g/l)	50	10	0	0.02	-10	10	40	25	0.5
Cd(μ g/l)	50	10	3.3	0.02	-6.7	6.7	40	16.75	0.335
Cu(μ g/l)	2000	1000	930	0.0005	-70	70	1000	7	0.0035
Zn(μ g/l)	3000	1000	340	0.00033333	-660	660	2000	33	0.011
Fe(μ g/l)	1000	100	77	0.001	-23	23	900	2.555555556	0.00255556
Hg(μ g/l)	60	10	0	0.01666667	-10	10	50	20	0.33333333
Mn(μ g/l)	300	100	10	0.00333333	-90	90	200	45	0.15
As(μ g/l)	50	10	0	0.02	-10	10	40	25	0.5
			Sum Wi	0.10183333				Sum $Wi \times Qi$	2.33538889
								HPI = WQi/Wi	22.9334424

VITA

I was born on August 09, 1994 in Gilgit Baltistan, Pakistan. I got my primary education from Aga Khan Dimond Jubilee School Gilgit and secondary school from Al ASR Public School Gilgit. For higher education I selected Karakoram International University and completed my bachelor degree on May 11, 2017 in Geology. After graduation, I started working with NBPFUNDS as Assistant Manager and after that I switched to FGPGMI after it I got admission at QAU Islamabad for my Master studies in September, 2020 and now ending up my Master studies with the completion this dissertation.

Turnitin Originality Report

HYDROGEOCHEMICAL CHARACTERIZATION OF GLACIAL-FED SURFACE WATER
RESOURCES IN THE CATCHMENT AREAS OF UPPER INDUS BASIN by Ammar
Yasir .



From CL DRSML (CL DRSML)

- Processed on 09-Feb-2023 14:34 PKT
- ID: 2010008080
- Word Count: 13765

Similarity Index

9%

Similarity by Source

Internet Sources:

6%

Publications:

7%

Student Papers:

2%

sources:

- 1 < 1% match (student papers from 20-Mar-2022)
[Submitted to Higher Education Commission Pakistan on 2022-03-20](#)
- 2 < 1% match (student papers from 29-Jun-2010)
[Submitted to Higher Education Commission Pakistan on 2010-06-29](#)
- 3 < 1% match (student papers from 25-Jun-2014)
[Submitted to Higher Education Commission Pakistan on 2014-06-25](#)
- 4 < 1% match (student papers from 20-Sep-2012)
[Submitted to Higher Education Commission Pakistan on 2012-09-20](#)
- 5 < 1% match (student papers from 29-Aug-2009)
[Submitted to Higher Education Commission Pakistan on 2009-08-29](#)
- 6 < 1% match (Internet from 08-Nov-2022)
https://www.researchgate.net/publication/292512557_Water_quality_Indicators_human_impact_and_environmental_health
- 7 < 1% match (Internet from 03-Feb-2023)
https://www.researchgate.net/publication/310831831_Monitoring_the_hygienic_quality_of_underground_water_in_different_localities_in_Egypt_and_Libya
- 8 < 1% match (Internet from 03-Feb-2023)
https://www.researchgate.net/publication/288138347_Studies_on_the_quality_of_groundwater_in_Madurai_Tamirnadu_India
- 9 < 1% match (Internet from 03-Feb-2023)
https://www.researchgate.net/publication/8527252_The_influence_of_pH_and_salinity_on_the_toxicity_of_heavy_metals_in_sediment_to_the_estuarine
- 10 < 1% match (Internet from 28-Jan-2023)
https://www.researchgate.net/publication/283456713_Assessing_Drinking_Water_Quality_in_Punjab_Pakistan
- 11 < 1% match (Internet from 19-Jan-2023)
<https://worldwidescience.org/topicpages/d/drinking+water+fluoridation.html>
- 12 < 1% match (Internet from 16-Jan-2023)
<https://worldwidescience.org/topicpages/w/water+bottle+samples.html>
- 13 < 1% match (Internet from 17-Jan-2023)
<https://worldwidescience.org/topicpages/p/plant+metal+concentrations.html>
- 14 < 1% match (Internet from 17-Jan-2023)
<https://worldwidescience.org/topicpages/q/queens+university+kingston.html>
- 15 < 1% match (Internet from 16-Jan-2023)
<https://worldwidescience.org/topicpages/e/estimated+drinking+water.html>
- 16 < 1% match (Narsimha Adimalla, "Groundwater Quality for Drinking and Irrigation Purposes and Potential Health Risks Assessment: A Case Study from Semi-Arid Region of South India", Exposure and Health, 2018)
[Narsimha Adimalla, "Groundwater Quality for Drinking and Irrigation Purposes and Potential Health Risks Assessment: A Case Study from Semi-Arid Region of South India", Exposure and Health, 2018](#)
- 17 < 1% match (Internet from 25-Dec-2017)
http://ntuhist.ac.in/web/bulletins/110_2015_proceedings.pdf
- 18 < 1% match (Internet from 27-Oct-2021)